TKE AND DIMPLE DESIGN: EXPLORING THE SYNERGISTIC EFFECT OF DRAG REDUCTION ON AHMED BODY.

SITI NUR NABILAH ABD RAZAK

B0920110051

BACHELOR OF MECHANICAL ENGINEERING TECHNOLOGY IN AUTOMOTIVE WITH HONOURS

2024

Faculty of Mechanical Technology and Engineering

TKE AND DIMPLE DESIGN: EXPLORING THE SYNERGISTIC EFFECT OF DRAG REDUCTION ON AHMED BODY.

Siti Nur Nabilah Abd Razak

Bachelor of Mechanical Engineering Technology in Automotive with Honours

2024

TKE AND DIMPLE DESIGN: EXPLORING THE SYNERGISTIC EFFECT OF DRAG REDUCTION ON AHMED BODY.

SITI NUR NABILAH ABD RAZAK

A thesis submitted

in fulfillment of the requirements for the degree of

Bachelor of Mechanical Engineering Technology in Automotive with Honours

Faculty of Mechanical Technology and Engineering

UNIVERSITI TEKNIKAL MALAYSIA MELAKA

2024

UNIVERSITI TEKNIKAL MALAYSIA MELAKA

BORANG PENGESAHAN STATUS LAPORAN PROJEK SARJANA MUDA

TAJUK: **TKE AND DIMPLE DESIGN : EXPLORING THE SYNERGISTIC EFFECT OF DRAG REDUCTION ON AHMED BODY.**

SESI PENGAJIAN: **2024-2025 Semester 1**

Saya **SITI NUR NABILAH ABD RAZAK**

mengaku membenarkan tesis ini disimpan di Perpustakaan Universiti Teknikal Malaysia Melaka (UTeM) dengan syarat-syarat kegunaan seperti berikut:

1. Tesis adalah hak milik Universiti Teknikal Malaysia Melaka dan penulis.
2. Perpustakaan Universiti Teknikal Malaysia Melaka dibenarkan membuat salinan untuk tujuan pengajian sahaja dengan izin penulis.
3. Perpustakaan dibenarkan membuat salinan tesis ini sebagai bahan pertukaran antara institusi pengajian tinggi.
4. **Sila tandakan (✓)

☐	TERHAD	(Mengandungi maklumat yang berdarjah keselamatan atau kepentingan Malaysia sebagaimana yang termaktub dalam AKTA RAHSIA RASMI 1972)
☐	SULIT	(Mengandungi maklumat TERHAD yang telah ditentukan oleh organisasi/badan di mana penyelidikan dijalankan)
☑	TIDAK TERHAD	

Disahkan oleh:

_____ _____

Alamat Tetap : Cop Rasmi :

Tarikh: 10 JANUARY 2025 Tarikh: 10 JANUARY 2025

** Jika tesis ini SULIT atau TERHAD, sila lampirkan surat daripada pihak berkuasa/organisasi berkenaan dengan menyatakan sekali sebab dan tempoh laporan PSM ini perlu dikelaskan sebagai SULIT atau TERHAD.

DECLARATION

I declare that this Choose an item. entitled " Tke And Dimple Design : Exploring The Synergistic Effect Of Drag Reduction On Ahmed Body " is the result of my own research except as cited in the references. The Choose an item. has not been accepted for any degree and is not concurrently submitted in candidature of any other degree.

Signature :

Name : Siti Nur Nabilah Abd Razak

Date : 10 / 1 / 25

APPROVAL

I hereby declare that I have checked this thesis and in my opinion, this thesis is adequate in terms of scope and quality for the award of the Bachelor of Mechanical Engineering Technology in Automotive with Honours.

Signature :

Supervisor Name : Ts. Mohd Faruq bin Abdul Latif

Date : 10 / 1 / 25

DEDICATION

This thesis are dedicated to :

My one and only creator, Allah,

To my beloved parents, Abd Razak bin Abd Aziz and Norenshah binti Abdul Wahab, whose boundless love, immense sacrifices, and unwavering belief in me have been the pillars of my strength. Your endless support and encouragement have been the driving force behind my every achievement. Your dedication and faith have inspired me to reach heights I never thought possible.

This thesis is dedicated to my supervisor, Ts. Mohd Faruq bin Abdul Latif, whose unwavering guidance and invaluable support have illuminated my path throughout this research journey. Your expertise and constant encouragement have been a beacon, steering me through challenges and ensuring the successful completion of this work. Your mentorship has profoundly shaped my academic and personal growth.

Finally, to everyone involved in this project, your contributions and support have been the silent yet powerful forces behind this endeavor. Thank you for standing by me and for being a part of this incredible journey. Your collective efforts and encouragement have made this accomplishment possible.

ABSTRACT

The goal of drag reduction in aerodynamics has long been a research focus, with consequences ranging across several disciplines, including the automobile and aviation industries. Surface alterations, such as dimples, have received attention as an emerging technology due to their ability to reduce drag. This thesis investigates the synergistic relationship between Turbulent Kinetic Energy (TKE) and dimple design, specifically in the context of the Ahmed body, a standard model in vehicle aerodynamics. This study analyzes how dimple design and TKE modification interact to reduce drag through a thorough examination, historical insights, and fundamental investigations. The Ahmed body, developed by S. R. Ahmed in 1984, serves as a standardized model for controlled experimentation, allowing for systematic testing of drag-reducing measures. Dimples, which are known for their drag-reducing potential via boundary layer turbulence, are investigated for their ability to modify TKE levels and alter flow separation patterns. Despite major advances in drag reduction approaches, there is still a significant vacuum in the research concerning the combined impacts of dimple design and TKE control on bluff bodies such as the Ahmed Body. This thesis seeks to close the gap by investigating how dimple designs interact with TKE to reduce drag on the Ahmed body. Using Computational Fluid Dynamics (CFD) simulations and experimental validation, the study methodically explores dimple geometry, turbulence dynamics, and drag coefficients to uncover unique insights into drag-reducing methods. The desired goals of this study are increased aerodynamic efficiency, decreased fuel consumption, and a lower environmental effect in transportation systems. By explaining the complex link between TKE and dimple design, this thesis aims to enhance aerodynamic optimization and technical innovation.

ABSTRAK

Selama bertahun-tahun, objektif untuk mengurangkan drag dalam aerodinamik telah menjadi subjek penyelidikan. Ini telah memberi kesan kepada pelbagai bidang, seperti industri penerbangan dan automotif. Lekukan, contoh perubahan permukaan, telah mendapat perhatian sebagai teknologi baru kerana keupayaannya untuk mengurangkan drag. Tujuan kajian ini adalah untuk mengkaji hubungan sinergistik antara Tenaga Kinetik Turbulen (TKE) dan reka bentuk lekukan. Penelitian ini difokuskan pada badan Ahmed, model standard dalam aerodinamik kenderaan. Untuk mengurangkan drag, kajian ini melihat bagaimana reka bentuk lekukan dan modifikasi TKE berfungsi bersama. Ia melakukan pemeriksaan menyeluruh, kajian sejarah, dan penyelidikan asas. S. Ahmed mencipta Badan Ahmed. Pada tahun 1984, Ahmed mencipta model untuk eksperimen terkawal dan membolehkan pengujian sistematik langkah-langkah pengurangan drag. Lekukan, yang dikenali kerana keupayaannya untuk mengurangkan drag melalui turbulensi lapisan sempadan, dikaji untuk keupayaannya untuk mengubah corak pemisahan aliran dan tahap TKE. Walaupun terdapat kemajuan besar dalam teknik pengurangan drag, penyelidikan mengenai kesan reka bentuk lekukan dan kawalan TKE pada Badan Ahmed masih terhad. Mencari cara reka bentuk lekukan berfungsi dengan TKE untuk mengurangkan drag pada badan Ahmed adalah matlamat kajian ini. Kajian ini mengkaji geometri lekukan, dinamik turbulensi, dan pekali drag untuk mendapatkan pemahaman yang berbeza tentang teknik pengurangan drag melalui simulasi dinamik bendalir berkomputer (CFD) dan pengesahan eksperimen. Kajian ini bertujuan untuk meningkatkan kecekapan aerodinamik, mengurangkan penggunaan bahan api, dan mengurangkan kesan sistem pengangkutan terhadap alam sekitar. Tesis ini bertujuan untuk meningkatkan optimisasi aerodinamik dan inovasi teknikal dengan menjelaskan hubungan rumit antara TKE dan reka bentuk lekukan.

ACKNOWLEDGEMENTS

I would like to thank my supervisor, Ts. Mohd Faruq bin Abdul Latif, for his important advice, support, and encouragement during this project. His skills and insight were invaluable in creating my thesis, and his patience and devotion encouraged me considerably.

I also want to express my deepest gratitude to Universiti Teknikal Malaysia Melaka (UTeM) for providing the essential resources and a favourable environment for my studies. The university's assistance and facilities were critical in allowing me to conduct my study effectively.

Special gratitude to my father, Abd Razak bin Abd Aziz, and mother, Norenshah binti Abdul Wahab, for their unfailing love, support, and sacrifice. Their unwavering support and confidence in my skills have been my driving factor throughout this journey.

Finally, I'd want to acknowledge and thank everyone engaged in this trip, whose efforts, large or small, have been critical to the completion of this thesis. Your help and assistance have been tremendously appreciated.

TABLE OF CONTENTS

LIST OF TABLES

LIST OF FIGURE

LIST OF SYMBOLS AND ABBREVIATIONS

TKE – Turbulent Kinetic Energy

WWII – World War II

CFD – Computational Fluid Dynamics

SLR – Systematic Literature Review

PRISMA – Preferred Reporting Items for Systematic Reviews & Meta Analysis

SHS – SuperHydrophobic Surfaces

DR – Drag Reduction

SCC – Semi Circular Cylinder

DNS – Direct Numerical Simulation

ABR – Axisymmetric Bodies of Revolution

ML – Machine Learning

CNN – Convolutional Neural Networks

ANN – Artificial Neural Networks

RF – Random Forests

WAM – Wall Attached Movements

OCF & CCF – Open & Close Channel Flows

RANS – Reynolds Averaged Navier Stroke

LES – Large Eddy Simulation

SGS – Sub Grid Scale

IDDES – Improved Delayed Detached Eddy Simulation

HST – High Speed Train

WRLES – Wall Resolved Large Eddy Simulation

WMLES – Wall Modelled Large Eddy Simulation

CL – Lift Coefficient

VIV – Vortex Induce Vibration

VG – Vortex Generator

.C_ϵ – Dissipation Coefficient

Re – Reynold Numbers

SBAB – Squareback Ahmed Body

PIV – Particle Image Velocimetry

FWMSC – Finite Wall Mounted Square Cylinder

SST – Shear Stress Transport

LDA – Laser Doppler Anemometry

ρ - fluid density,

U - characteristic velocity of the flow

L - characteristic length scale

M - dynamic viscosity of the fluid

u - fluid velocity vector

μ - dynamic viscosity of the fluid

μt - turbulent viscosity

σ_ε and σ_k - model constants

P_k - turbulent production term

$C_{1\varepsilon}$ and $C_{2\varepsilon}$ - model constants

ω - turbulence dissipation

Cp – Pressure Coefficient

Cd - Drag coefficients

LIST OF APPENDICES

Chapter 1

Introduction

1.1 Background

Drag reduction is a crucial aspect of aerodynamics research, having major implications for car design, aviation, and other fluid dynamics areas. Surface modifications, like as dimples, are a new technique to minimizing drag. This chapter gives a background research on TKE and dimple design, with a focus on their synergistic influence on drag reduction, particularly in the context of the Ahmed Body.

The research of drag reduction techniques stretches back to the dawn of the 20th century, with major developments achieved during and after WWII. The early focus was on simplifying forms to minimize resistance. However, it was not until the second half of the 20th century that researchers began to investigate the impact of surface textures on aerodynamic performance. Ludwig Prandtl, known as the "Father of Modern Aerodynamics," wrote one of the most famous early works in the field of study. Prandtl's boundary layer theory, established in 1904, paved the way for understanding how surface roughness and changes affect fluid flow (Ludwig Prandtl, “Motion of Fluids with Very Little Viscosity” (1904), n.d.)

S. R. Ahmed created the Ahmed body in 1984 as a smaller automotive prototype for studying vehicle aerodynamics. It has become an everyday reference model for vehicle aerodynamics because of its basic geometry and refined flow characteristics, such as flow separation and wake creation (Ahmed et al., 1984). This model lets researchers to systematically test a substitute drag reduction approaches in a controlled setting.

Dimples, which are widely associated with golf balls, have been extensively researched for their capacity to reduce drag by altering boundary layer flow. When applied on surfaces, dimples can cause turbulence in the boundary layer, therefore delaying flow separation and lowering pressure drag. The concept of employing dimples in aerodynamics attracted significant interest in the late 20th century, with many research investigating their effect on varied forms and flow conditions. (Choi & Choi, 2002).

TKE is an indicator that describes the level of turbulence in fluid flow. It indicates the amount of force contained in the turbulent eddies and is an important metric for understanding and modelling turbulent flows. TKE manipulation by surface alterations like as dimples can result in significant alterations to a body's aerodynamic properties. By raising turbulence at the surface, dimples can boost TKE, which assists in maintaining a more connected flow and lowering total drag. (Stephen B Pope, 2001)

TKE and dimple design have mutually beneficial impacts on drag reduction due to the combination of produced turbulence and enhanced surface roughness. When appropriately built, dimples can increase TKE near the surface, influencing separation of flow and reattachment patterns. This combination can significantly reduce drag, making it an attractive field of research for increasing the aerodynamic efficiency of vehicles. (*An_Introduction_to_Computational_Fluid_D*, n.d.)

Understanding the interaction between TKE and dimple design is critical for creating efficient drag reduction solutions. The historical backdrop and fundamental studies form the framework for present and future study in this field. As we progress through this thesis, we will look into particular approaches and analysis to analyze these impacts on the Ahmed Body, with the goal of contributing useful insights to the field of aerodynamic optimization.

1.2 Problem statement

Numerous drag-reducing measures, including surface modifications, particle characteristics, and riblet designs, have been thoroughly examined in fluid dynamics research. Turbulence models and flow properties in relation to various forms have also been studied. However, there is a large gap in the literature regarding the combined effects of TKE and dimple design on bluff bodies, such as the Ahmed Body. While drag-reducing tactics such as superhydrophobic surfaces and airflow alterations have been studied, the relationship between dimple design and TKE control on bluff bodies remains unclear (Ahmed et al., 1984).

The thesis, "TKE and Dimple Design: Exploring the Synergistic Effect of Drag Reduction on Ahmed Body," seeks to address this gap by looking at how dimple designs might work with TKE to minimize drag on Ahmed Body. Initial research suggests that dimpled surfaces can produce controlled turbulence in the boundary layer, influencing flow properties and TKE levels. This study will look at the interaction between dimple shape, turbulence, and drag coefficients to get fresh insights into drag reduction (Menter, 1994). Understanding these impacts may lead to the creation of more efficient and sustainable transportation systems, lowering fuel consumption and CO2 emissions through increased aerodynamic efficiency (*An_Introduction_to_Computational_Fluid_D*, n.d.)

1.3 Research question

From the problem statement, the research question is developed and described as follows:

1. How do different dimple designs impact the TKE levels around the Ahmed Body?
2. How does the combination of TKE control and dimple design influence flow separation and reattachment on the Ahmed Body?
3. What is the relationship between dimple geometry and drag reduction on the Ahmed Body?

1.4 Research Objective

This study aims to explore the effect of dimple design on the drag reduction of the Ahmed body. The specific goals of this study are:

1. To compare the aerodynamic performance of dimple-augmented Ahmed Bodies with conventional smooth-surface Ahmed bodies.
2. To validate Ahmed body by Computational Fluid Dynamics (CFD) study.
3. To analyze the effect of dimple augmentation on the top surfaces of the Ahmed body on turbulence kinetic energy and drag reduction.

1.5 Scope of Research

The scope of this research are as follows:

The project will thoroughly investigate how side dimples affect the aerodynamic performance of the Ahmed Body in the context of vehicle aerodynamics. It will largely focus on surface alterations made to the Ahmed Body, with a particular emphasis on side dimples, which serve as the core geometric model. The study will thoroughly explore differences in dimple properties, such as size, shape, and arrangement, in order to determine their influence on essential aerodynamic aspects. The primary factors under consideration will be skin friction drag and total drag coefficient, which will be fully evaluated using CFD simulations. These simulations will go through stringent validation methods to ensure their accuracy, which will include comparisons to validated experimental data or earlier CFD evaluations.

Given the challenges, the study will focus on the Ahmed Body as the major topic to extract insights that may be used to influence design techniques in a variety of vehicle applications in the automotive industry. Time restrictions, computing resources, and expertise will all be considered when determining the study scope. The primary goal is to guarantee that the research process stays viable, and resources are allocated efficiently throughout the investigation.

1.6 Hypothesis

This thesis, titled "TKE and Dimple Design: Exploring the Synergistic Effect of Drag Reduction on Ahmed Body," is likely to provide important insights into the aerodynamic performance of the Ahmed Body with dimple. It is expected that the inclusion of the dimples will greatly reduce friction drag, with the degree of reduction varied depending on the dimple properties. These modifications are projected to increase the Ahmed Body overall aerodynamic efficiency, resulting in a lower total drag coefficient.

The study goal is to determine the most efficient dimple configurations to minimize drag through unique designs, as well as to perform complete parametric research. The project intends to improve understanding of flow management methods in vehicle aerodynamics by learning more about the aerodynamic principles that drive drag reduction from dimples.

The validation of CFD simulations using experimental data or prior research will ensure the reliability of the computational method employed in the study. The anticipated results have the potential to affect the practical application of automotive aerodynamics, potentially leading to the development of novel techniques to improve vehicle performance, fuel efficiency, and environmental sustainability. Overall, the projected outcomes of this thesis indicate the prospect of furthering our understanding and use of aerodynamic improvements in vehicle engineering, hence contributing to breakthroughs in automotive technology.

Chapter 2

Literature Review

2.1 Introduction

In automotive aerodynamics, reducing drag on bluff bodies such as the Ahmed Body is critical to enhancing vehicle performance and efficiency. Recently, surface alterations like the design of dimples, which are modelled after naturally occurring aerodynamic characteristics like those seen on golf balls, have become a viable method for improving flow management and lowering drag.

Dimples affect the flow features surrounding the body and impact TKE by creating controlled turbulence in the boundary layer. The purpose of this literature review is to provide an overview of current understanding about the application of dimple design, especially for reducing drag on Ahmed Body. This review will look at experimental and computational inquiries to understand the mechanisms by which dimples influence drag coefficient and provide suggestions on improving dimple geometry and placement for best aerodynamic performance increase.

2.2 Systematic Literature Review (SLR)

A SLR is a rigorous and structured approach to synthesizing existing research relevant to a specific research question or topic (Kitchenham, 2004); (Tranfield et al., 2003). A well-defined research issue serves as the foundation for the methodical search approach, which entails thorough searches across several databases using certain search terms and criteria (Petticrew & Roberts, 2006). Research articles found via the search are filtered according to predetermined inclusion and exclusion standards, and the relevance of each study is evaluated separately by multiple reviewers (Citations-20240610T140056, n.d.).

Key information, including study design, methodology, and findings, are methodically retrieved and synthesized during the data extraction process of selected studies (Martyn-St James et al., 2021). Quality assessment tools are often applied to evaluate the reliability and validity of included studies (Downs & Black, 1998). Following a transparent presentation of the synthesized results, important discoveries are summarized, implications are discussed, and gaps in the literature are noted (Grant & Booth, 2009). In general, the goal of a systematic literature review is to present a thorough and objective overview of the state of knowledge currently available on a particular subject, providing insightful information for practice, research, and policy development.

2.2.1 Identifying Keyword

In the initial step of conducting a SLR, identifying keywords related to the main topic is crucial for developing an effective search strategy (Kitchenham, 2004), (Petticrew & Roberts, 2006). This involves carefully selecting and refining specific terms and phrases that accurately represent the research question. Keywords are typically derived from key concepts within the research topic and can include synonyms, related terms, and variations of terminology used in the field (Tranfield et al., 2003).

The process begins with brainstorming potential keywords based on the research question, followed by consulting relevant literature and databases to identify commonly used terms and terminology variations (*Citations-20240610T140056*, n.d.). For this paper, I chose two main phrases as my keywords which are "turbulent kinetic energy" and "aerodynamic efficiency." Identifying and utilizing appropriate keywords helps enhance the precision and comprehensiveness of search queries (Grant & Booth, 2009). This step lays a critical foundation for the subsequent stages.

2.2.2 Synonym of Keyword

Following the identification of keywords for a SLR, the next essential step involves searching for synonyms and related terms to expand and refine the search strategy (Petticrew & Roberts, 2006), (*Citations-20240610T140056*, n.d.). Synonyms are alternative words or phrases that convey similar meanings to the identified keywords and are important for capturing a comprehensive range of relevant literature (Tranfield et al., 2003). Searching for synonyms helps broaden the scope of the literature search by considering different terminology used across various disciplines and contexts.

I consult thesauruses to generate a list of relevant synonyms for my phrase and I get "TKE" and "drag reduction" for the synonyms of my keywords respectively (Grant & Booth, 2009) By incorporating synonyms into the search strategy, I can maximize the retrieval of pertinent studies and ensure a more thorough examination of the available literature during the systematic review process.

Table 2.1 Synonym of Keyword

Keyword	**Synonym**
Dimple	Divot, Cleft, Concavity, Dent
TKE	Turbulence Kinetic Energy
Drag Reduction	Aerodynamic Efficiency

2.2.3 Construct Search String for Specific Search Engine

Following the identification of keywords and synonyms, the next step in a SLR is to construct a well-defined search string (Petticrew & Roberts, 2006), (*Citations-20240610T140056*, n.d.). This involves organizing and combining the identified terms using Boolean operators (such as AND, OR, NOT) to create a structured query for database searches. The search string aims to maximize the retrieval of relevant literature while minimizing irrelevant results by specifying logical relationships between terms. Combining synonyms with OR broadens the scope of the search, ensuring that variations of key concepts are included. On the other hand, using AND between different keywords narrows down the search to articles that contain all specified terms, refining the relevance of retrieved documents.

I personally use two specific search engines which are Scopus and Web of Science. The string that is developed for Scopus is (ALL(TKE OR “Turbulence Kinetic Energy”)) AND ("Drag Reduction" OR "Aerodynamic Efficiency") while for Web of Science, the search string becomes TS=((TKE OR Turbulence Kinetic Energy) & ("Drag Reduction" OR "Aerodynamic Efficiency")). By constructing a well-crafted search string, the efficiency and accuracy of the literature search process could be optimize, facilitating the identification of studies that address the research question.

Table 2.2 Table of Search String

Search Engine	Search String
Scopus	(ALL(TKE OR “Turbulence Kinetic Energy”)) AND ("Drag Reduction" OR "Aerodynamic Efficiency")
Web of Science	TS=((TKE OR Turbulence Kinetic Energy) & ("Drag Reduction" OR "Aerodynamic Efficiency"))

2.2.4 Preferred Reporting Items for Systematic Reviews and Meta-Analysis (PRISMA)

The PRISMA method is a guideline for systematic reviews and meta-analyses, ensuring clear and reliable research (Moher David AND Liberati, 2009). It provides a checklist of important items, like why the review is needed, how studies are chosen, and how data is analyzed. Following PRISMA helps researchers conduct thorough and trustworthy reviews by organizing the review process (Page et al., 2021) It's essential for anyone aiming to do careful and comprehensive literature reviews. In figure 2.1 shown the flowchart of the thesis PRISMA process.

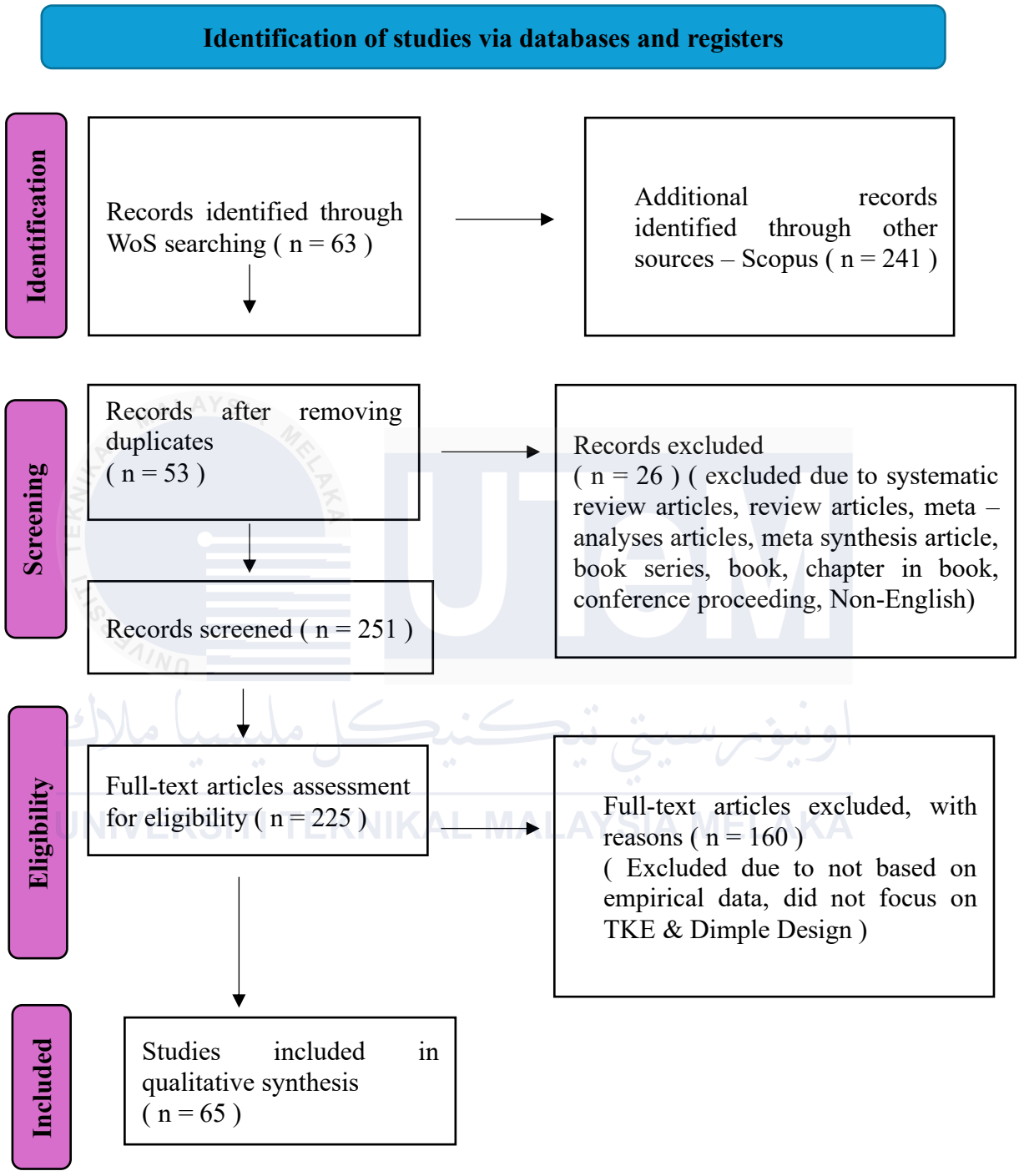

Figure 1.1 Preferred Reporting Items for Systematic Reviews and Meta-Analysis Flow Chart

2.2.4.1 Identification

The identification phase, guided by PRISMA guidelines, aims to minimize bias, enhance transparency, and establish a reliable foundation for the subsequent stages of the systematic review or meta-analysis. During this phase, this developed a comprehensive search strategy tailored to the research question, identifying relevant keywords, synonyms, and search terms based on key concepts.

Scopus and Web of Science is selected as search engines and execute search queries using Boolean operators to combine keywords and refine search parameters. Whereby from web of science 63 journal are identified and 241 journals from Scopus are found. Transparent reporting of the search strategy is essential for ensuring the reproducibility and transparency of the systematic review process (Page et al., 2021)

2.2.4.2 Screening

The screening phase in the PRISMA method is a crucial stage where process of systematically evaluate the titles and abstracts of retrieved studies to identify potentially relevant literature. This phase involves applying predefined inclusion and exclusion criteria, considering factors such as study design, participant characteristics, interventions, outcomes, and relevance to the research question. Studies that meet the initial screening criteria undergo a detailed full-text review to confirm eligibility for inclusion in the systematic review or meta-analysis.

Transparent documentation of the screening process, including reasons for excluding studies, is essential for ensuring the reliability and reproducibility of the review (Shea et al., 2017). By following standardized screening procedures within the PRISMA framework, researchers minimize bias, enhance rigor, and provide a clear rationale for study selection in the final systematic review or meta-analysis.

From the first part of screening, 53 journals are removed due to duplicates from both of the search engines. Then the records are screened until 251 journals excluding systematic review articles, meta analysis articles, books and conference proceeding.

2.2.4.3 Eligibility

The eligibility phase within the PRISMA method is a crucial stage where I meticulously assess the full text of potentially relevant studies identified during screening. This phase involves reviewing each study in detail to determine if it meets specific inclusion criteria related to study design, participant characteristics, intervention/exposure, comparator, outcomes, and relevance to the research question.

I rigorously scrutinize study methods, results, and conclusions to ensure alignment with the review's objectives and the validity of the evidence. Quality assessment or risk of bias appraisal may also be conducted to evaluate methodological rigor and internal validity. Transparent documentation of eligibility decisions and reasons for study inclusion or exclusion is essential for ensuring the integrity and reproducibility of the systematic review. (Moher David AND Liberati, 2009). From the records screened before, it is then reduce until 225 for the full text article assessment for eligibility and the amount excluded in total of 160 journals.

2.2.4.4 Included

In the included phase of the PRISMA method, I finalize the selection of studies for my systematic review or meta-analysis. I carefully document and list the chosen studies, describing each study's details and findings. During this phase, I extract important information from selected studies, such as study design, participant characteristics, interventions, outcomes, and results.

Depending on the research goals and data availability, this phase may also involve synthesizing the data through qualitative or quantitative methods like meta-analysis. The aim is to systematically analyze and summarize the findings of these studies to address the research question or objectives of the review. Following the PRISMA guidelines ensures transparency and reliability in reporting the outcomes of the systematic review or meta-analysis. After all the steps that have been taken, the total studies included for this paper is 63 papers.

2.3 Background Study

In recent years, the field of aerodynamics has witnessed significant advancements driven by ongoing research and innovation. As the demand for improved vehicle performance and efficiency continues to grow, there has been a particular focus on exploring novel approaches to reduce drag and enhance aerodynamic performance.

This background study aims to provide a detailed overview of key concepts, theories, and findings relevant to the interaction between TKE and dimple design in the context of drag reduction on Ahmed Body configurations.

The rationale behind this study lies in the need to consolidate and evaluate diverse perspectives on the synergistic effect of TKE and dimple design on drag reduction. By exploring the existing literature, this thesis aims to identify gaps, inconsistencies, and emerging trends that can guide future research directions in the field of aerodynamics and vehicle design.

The following sections will delve into the foundational aspects of TKE, dimple design, and their interaction with drag reduction on Ahmed Body configurations, providing insights into the evolution of research in this domain and setting the stage for a comprehensive investigation into the research questions posed by this study. Figure 2.2 show the flow of the journal obtain from year 2019 to 2024 from the PRISMA method.

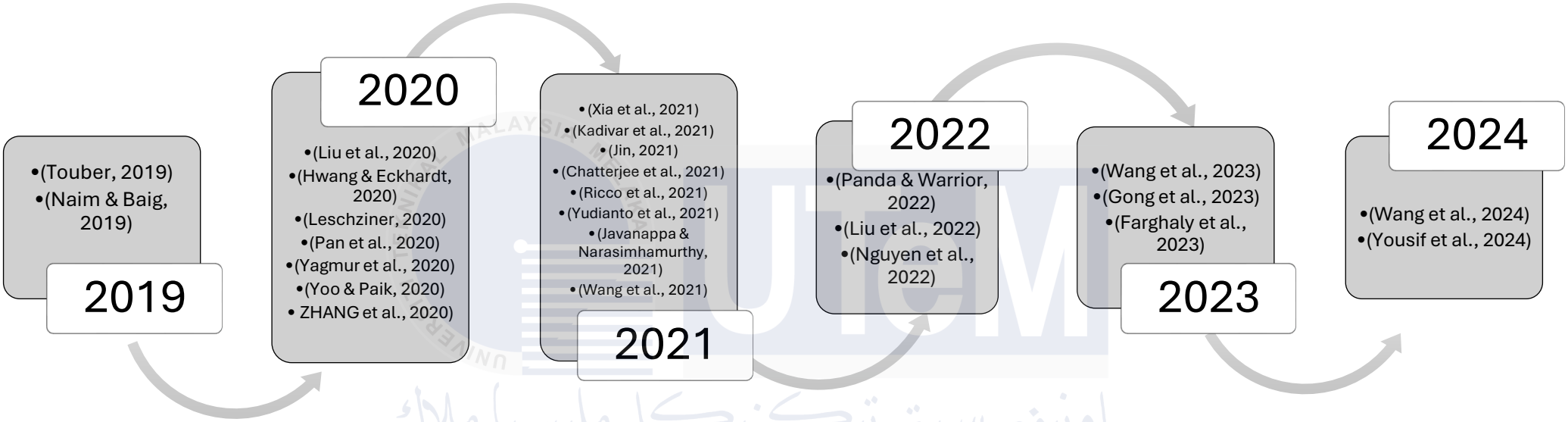

Figure 2.2 Flowchart Journal Obtain from PRISMA

2.3.1 Year 2019

In 2019, Relevant aspects of turbulent flow dynamics and their effects are highlighted by the studies that are discussed. Research on the application of SHS to DR in Taylor-Couette flow shows promising results, with streamwise-aligned SHS generating up to 34% DR. (Touber, 2019)

Meanwhile, the analysis of bulk-to-shear viscosity ratios in turbulent carbon dioxide flows underscores the impact of neglected factors on predicting aerothermal loads. This research identifies distinct regimes in the Navier-Stokes equations revealing complex interactions between dilatational and solenoidal kinetic energy (Naim & Baig, 2019). The way that variable particle properties (such as size and density) influence turbulent structures at varying temperatures and bridging insights from particle-laden flows and thermally stratified environments.

2.3.2 Year 2020

From this particular year, there are more researchers that studies relatively about drag reduction related to TKE. Firstly, In a particle-free flow, the mean flow consumes more than half of the input energy, with the remaining portion sustaining turbulence. In contrast, the energy required for mean flow and turbulence in a particle-laden flow is comparable to that of an unladen flow, but the amount of turbulence produced is much less. (Pan et al., 2020)

Concerns about the environment and the desire to use less fuel for transportation are the driving forces behind the quest to reduce drag. With turbulent friction accounting for almost half of the drag during flight, it is a significant factor in aviation. Although difficult to implement, altering the motion of walls in planes has drawn interest because it provides notable savings in drag. (Leschziner, 2020)

Next, there are also articles that examine how riblets (small grooves on a wing) can reduce drag while the wing is flying at a low speed. The study investigates the effects of wing form on riblet function. In order to comprehend how these grooves lessen drag, it looks at how the airflow over the wing surface is altered by them. The study adds to our understanding of how riblets can increase the efficiency of wings when flying at slower speeds. (ZHANG et al., 2020)

The present study explores, from an altered perspective, Townsend's model of related eddies in boundary layers. There are variations related to the primary profile in the velocity field. Although the primary profile is obtained through complex mathematics, the variations are depicted through more straightforward techniques that involve turbulent diffusion and unpredictable impacts. This method, which uses the same general notion as the original attached eddy model, simplifies the solution of the fluctuation equations. (Hwang & Eckhardt, 2020)

In the present study, airflow around a SCC, a significant geometry in fluid mechanics, is analyzed using computer simulations. Utilizing various computer models, the researchers were able to forecast properties such as turbulence energy, vorticity, and velocity patterns. The amount of drag the SCC encounters and the airflow's symmetry are the main subjects of the research. This work contributes to a better understanding of aerodynamics around the SCC and other basic forms. (Yagmur et al., 2020)

The study discusses the application of computer models to high-speed fluid flow studies in engineering. Scholars are investigating various techniques for accurately predicting the flow of fluids near walls. A variety of turbulence models are being tested to see which performs best for key parameters such as viscosity and turbulence energy. Enhancing computer simulations for engineering applications involving fluids moving quickly is the aim. This work contributes to the assurance that simulations offer accurate data regarding fluid behaviour in real-world situations. (Yoo & Paik, 2020)

The subject matter studies the movement of heat through supercritical water turbulent flows at various pressures using computer models. The goal of the study is to determine how these circumstances alter fluid characteristics and how heat transmission is impacted. They discovered that turbulence along the flow route reduces at lower pressure ratios, where fluid characteristics fluctuate more. The research demonstrates that significant variations in fluid density significantly affect the reduction of heat transmission and turbulence. (J. Liu et al., 2020)

2.3.3 Year 2021

Scientific studies on technology that can reduce drag for vehicles on roads, trains, in the air, and on water have been driven by the need to reduce fuel consumption and CO2 emissions in transportation. Since skin-friction drag accounts for almost half of total drag during a cruise, it is a major area of focus for civil aviation. Researchers are looking into techniques to lessen turbulence close to the surface in order to reduce drag since turbulence influences skin friction. (Ricco et al., 2021)

Numerous approaches to model validation are presented, with an emphasis on comparing industrial scenarios with real-world tests. It is emphasized how crucial it is to use physical trials to validate models. Next, the application of a turbulence model is investigated for particular flow problems in metallurgical processes, like electromagnetic turbulence suppression, bubble-induced turbulence, and supersonic jet transport. (Y. Wang et al., 2021)

Researchers examined the differences in the flow of water surrounding a barrier with a dipped surface. To reduce flow separation, the barrier was designed to resemble an airfoil with a flat top and particular slopes on its sides. The water surface was lowered above the obstruction to allow the researchers to see variations in the flow pattern. They distinguished three principal flow regions: the region upstream, downstream, and over the obstacle's crest.(Chatterjee et al., 2021)

The aim of the research was to better understand how energy is transferred and conserved in fluid flow, as well as how cavitation arises around a flat hydrofoil. When TKE falls below a certain pressure, vapor bubbles develop, and a process known as cavitation takes place. TKE is absorbed by cavitation as it develops and is transformed into phase-change energy, which modifies the flow field's pressure distribution. Cavities may collapse as a result of this pressure shift, producing re-entrant jets or vortex formations. The cycle returns when cavitation bubbles burst, releasing energy back into the flow. (Jin, 2021)

This review focuses on fundamental hypotheses concerning the differences in flow between smooth and rough surfaces, summarizing both new and previous studies. Future research in areas such as manufacturing and aerodynamics will benefit from the discoveries, but obstacles still exist because of the variety of rough surface types and how they affect flow dynamics. (Kadivar et al., 2021)

In this study, turbulent flow in a straight Couette channel with a top wall that is smooth and flows at a constant speed and a bottom wall that is roughened by square ribs is examined using DNS. The roughness elements have distinct streamwise pitches that divide them apart. TKE in the flow is increased by the roughness, which increases turbulence near both smooth and rough walls. (Javanappa & Narasimhamurthy, 2021)

This work investigates the effects of particles on turbulent flows in designs with downward channels using simulations. Researchers look at how fluid-turbulence interactions are affected by particle size, density ratio, and settling rate. Their main goal is to comprehend the behaviour and dispersion of particles in the flow under various circumstances. Important discoveries include variations in the distribution and severity of turbulence depending on the properties of the particles and the direction of flow, offering insights into the fluid-turbulence dynamics in particle-laden systems. (Xia et al., 2021)

The study focuses on how buses moving in a platoon's aerodynamic performance is impacted by crosswinds. It studies how crosswind circumstances affect aerodynamic coefficients such as lift force, drag force, side force, and pressure coefficient. When no crosswind was taken into account in terms of the created turbulent kinetic energy of the leading and following buses, the benefits of the platoon structure were explained in further detail. (Yudianto et al., 2021)

2.3.4 Year 2022

The study used streamwise vorticity and TKE computations to examine the causes of secondary flows in partially filled pipes. It was discovered that secondary flows begin at the corners, where turbulence is active, where the pipe wall meets the free surface. Asymmetric turbulence also produces additional vorticity close to the centerline of the free surface. In comparison to fully filled pipes, pipes that are half or three-quarters full have less overall friction due to the dispersive stresses created by these secondary flows, which lessen turbulent shear stress. (Y. Liu et al., 2022)

In engineering design, accurate and efficient airflow models around ABR have been a major goal. In order to forecast the flow patterns over ABR, this paper investigates the application of ML techniques such as CNN, ANN, and RF. ML models that have been trained are used to replace conventional CFD techniques. (Panda & Warrior, 2022)

The exploration of superhydrophobic drag reduction has been and continues to be of significant interest to various industries. In the present work, DNS is utilized to investigate the effect of the parameters on the drag-reducing performance of SHS. Simulations with a friction Reynolds number of 180 were carried out at solid fraction and three distribution shapes: aligned, staggered, and random. The top wall is the smooth one, and the bottom wall is a SHS. (Nguyen et al., 2022)

2.3.5 Year 2023

Improving heavy-duty vehicle aerodynamic efficiency is a major concern for the automobile industry to reduce fuel consumption. The goal of this study was to enhance vehicle profiles by integrating various drag reduction technologies and evaluating their effects through computational and experimental research. The additional devices are truck caps with varied angles, gap devices with variable lengths, and flat flaps with different diameters and angles. (Farghaly et al., 2023)

Direct numerical simulations were performed to investigate the behaviour of WAMs in OCFs and CCFs with two distinct friction Reynolds numbers (550 and 1000). Extremely large domain sizes (24–48 times the height of the channel along the streamwise direction) were used to fully catch the largest and most energetic WAMs. The study's main objective was to employ a linear coherence spectrum analysis to examine the properties and traits of WAMs, such as their geometry and motion patterns. (Gong et al., 2023)

This study looks at how airflow in transportation routes is affected by piston wind from cage lifting in an air intake shaft. We examine the characteristics of airflow turbulence and investigate how the piston wind impact affects the flow using the turbulence model and dynamic mesh simulations. The wind speed in the roadway under piston wind, according to the results, has a normal distribution. Along the length of the roadway, the intensity of the turbulent flow displays self-similar behaviour with an overall exponential distribution. Under the effect of piston wind, the intensity of the turbulent flow is symmetrically distributed down the centerline of the roadway. (X. Wang et al., 2023)

2.3.6 Year 2024

This study examines turbulent airflow close to a surface using cutting-edge imaging methods. The goal of gathering velocity data at various scales is to help the researchers comprehend the behaviour of turbulence in this airflow. They divide the velocity fluctuations into several sizes using a technique known as wavelet transforms, and then they analyze the distribution of turbulence energy along these scales. The study also examines the effects of particular turbulent patterns on turbulence statistics and airflow behaviour as a whole. Finding typical turbulent structures and their effects on airflow dynamics is the ultimate objective. (Q.-X. Wang et al., 2024)

This paper investigates the optimization of airflow around a FWMSC using plasma actuators. Researchers test plasma actuators placed on various cylinder surfaces in a tiny wind tunnel. Their goal is to determine how these actuators affect the behaviour of the airflow by varying their voltage and frequency. In order to evaluate the efficiency of the plasma actuators, drag force measurements are made and airflow patterns are shown using methods such as PIV. The study's overall goal is to show how plasma actuators can improve the aerodynamic efficiency of the cylinder by reducing flow separation and turbulence behind it.(Yousif et al., 2024)

2.4 Modelling

This thesis modelling section focuses on investigating drag reduction techniques and turbulent flow dynamics as they relate to the Ahmed Body, a key model in automotive aerodynamics. The aerodynamic performance of vehicles is greatly influenced by turbulence, which also affects flow stability, lift, and drag. In order to optimize vehicle design and increase overall economy, it is imperative to comprehend the distribution and behaviour of TKE.

2.4.1 Reynolds-Averaged Navier-Stokes (RANS)

RANS modelling technique is used to simulate turbulent flows. The mean flow and turbulent fluctuations are distinguished in RANS by averaging the Navier-Stokes equations, which regulate fluid motion. Turbulence models such as the k-epsilon or k-omega models are used to model Reynolds stresses and other factors that reflect the effects of turbulence in the resulting equations. RANS is frequently used in engineering applications to forecast flow behaviour, pressure distribution, and other flow properties. It is efficient in simulating steady or time-averaged turbulent flows. RANS's accuracy for turbulent flows that are unstable or extremely complex may be limited because it relies on the assumption that turbulence effects are statistically steady.

2.4.2 Large Eddy Simulation (LES)

A CFD method called LES is used to model turbulent flows. There are big and small scales of motion in the computational domain of LES. The Navier-Stokes equations are directly used to resolve the large scales, which contain the majority of the turbulent flow's energy, while sub grid-scale models are used to describe the smaller and less energetic scales.

LES is employed when a high level of detail is required to resolve flow features and is especially useful for capturing big, coherent structures in turbulent flows. It can offer light on intricate flow processes like turbulent jet mixing or vortex shedding behind bluff bodies.

2.5 Methodology

In this research, I examine the approaches used in earlier research on TKE and drag reduction in the context of automotive engineering in this overview of the literature. My objective is to investigate the methods used by researchers to simulate and analyze turbulent flows in order to reduce drag and improve the aerodynamics of vehicles. In hope to uncover common approaches, assess their effectiveness, and learn more about the relationship between TKE and drag reduction tactics in the automotive sector by looking into the methodologies used in these studies. This paper gives a general overview of the techniques used to evaluate drag characteristics, investigate novel ways to increase vehicle efficiency through aerodynamic upgrades, and research TKE distribution.

No.	Author	Method	Turbulence Model	Input	Output
1	(Vashishtha et al., 2019)	• Decaying homogeneous • Isotropic turbulence.	Large eddy simulations (LESs)	• Direct numerical simulation (DNS) • LES	Establish the suitability of our renormalized viscosity scheme for LES.
2	(Lu et al., 2019)	RANS equations on structured grids over the inlet Mach	Reynolds-averaged Navier–Stokes (RANS)	Spherical dimples are embedded along chord of suction surface.	Two dimple configurations can both reduce the total pressure loss in all researched Mach number
3	(Ramirez-Pastran & Duque-Daza, 2019)	A standard smooth-wall channel	Large-Eddy Simulations (LES)	Standard channel flow case at four different friction Reynolds numbers	Implementations of the SGS models were successful in predicting the turbulent behaviour of the selected flow cases.
4	(Toloui et al., 2019)	Using digital inline holographic particle tracking velocimetry	-	Turbulent flow and roughness deformation are measured	TKE is dampened and converted into streamwise deformation of roughness.
5	(J. Wang et al., 2020)	Revealing aspects to further improve the HST aerodynamic performance.	Improved delayed detached eddy simulation (IDDES)	The underbody flow, slipstream velocity, aerodynamic drag and the computational costs	The turbulence kinetic energy differences with different cases.

6	(Marimuthu & Chinnathambi, 2020)	Studies on the sharkskin pattern,	-	Performance of the butterfly valve is improved.	The skin friction coefficient, turbulence kinetic energy and outlet velocity of the butterfly valve.
7	(Hesse & Morgans, 2021)	Flow around a 1/4 scale squareback Ahmed body.	Large eddy simulation (LES)	Re_H=33,333	Front separation bubbles, of the Ahmed body nose generate high levels of TKE through the shedding of large hairpin vortices.
8	(Yudianto et al., 2021)	-	Computational Fluid Dynamic (CFD)	Yaw angle from 0° to 30° and coefficient X/L from 0.05 to 1.25	Comparison between the numerical study and experiment indicated a satisfactory correlation of results validation.
9	(Panda & Warrior, 2022)	ABR is predicted using machine learning (ML) algorithms.	Computational fluid dynamics (CFD)	High fidelity Reynolds stress transport model.	ML-based surrogate model predictions are as accurate as CFD results.

10	(Feng & Zhang, 2022)	The plate and wind turbine are coupled on the rear of the vehicle.	Reynolds Average Navier-Stokes（RANS）	Reynolds number Re=1. 43×10^6	The drag reduction effects of the plate and the wind turbine increase first and then decrease with the increase of the plate length.
11	(Mondal et al., 2023)	Develops a computational model to investigate fluidic on-demand winglets.	-	The turbulence parameters such as TKE and turbulent dissipation rate .	The implementation of fluidic winglets leads to a significant reduction in drag.
12	(H. Wang et al., 2023)	Direct numerical simulations of turbulent flow.	-	Reynolds number	Insight into the physics of flow over C-D riblets and may contribute to the further development of this flow control strategy.
13	(Jaffar et al., 2023)	ANSYS-Fluent	-	Reynolds number and different angles of attack.	This reduction in the turbulence kinetic energy implies that the near-wake high energy structures are mitigated.

Table 2.3 Summary Methodology of Literature Review

From the table above, we could see each article have a detail method with their own input to gain the appropriate output. Firstly, using a renormalized viscosity framework, LES of decaying homogeneous and isotropic turbulence were carried out, and their results were compared with DNS. The determined scales of DNS were matched with a range of grid resolutions, demonstrating good agreement in kinetic energy flow, kinetic energy spectrum, and turbulence kinetic energy between LES and DNS. The study proves that the renormalized viscosity technique works well for LES applications. (Vashishtha et al., 2019)

Compatible averaged by Reynolds Navier-Stokes equations are solved on structured grids in order to examine the flow properties of compressor cascades with dimples. They study two different suction surface spherical dimple shapes over a range of inlet Mach values. Due to enhanced TKE within the boundary layer, the numerical simulation assesses the suppression of separation bubbles and the reduction of total pressure loss. (Vashishtha et al., 2019)

SGS models for LES are evaluated using CFD for wall-bounded flows. The study compares SGS models with available DNS data at different Reynolds numbers, analyzing mean flow profiles, turbulent statistics, and profiles of TKE. (Ramirez-Pastran & Duque-Daza, 2019)

The use of digital inline holographic particle tracking velocimetry is examined for turbulent channel flows across rigid and flexible roughness surfaces. The study shows decreases in Reynolds stresses and coherent flow patterns across flexible roughness compared to rigid surfaces by measuring turbulent flow and roughness deformation simultaneously. (Toloui et al., 2019)

Utilizing IDDES, the aerodynamic performance of a HST featuring bogie cavities is investigated. By putting in bogies around cavities or caulking them, the numerical analysis shows effects on slipstream velocity distribution and TKE, which significantly reduce drag. (J. Wang et al., 2020)

The performance increase of butterfly valves with biomimetic surface patterns is analyzed through computational simulations. Improvements in TKE, outlet velocity, and skin friction coefficient are demonstrated by the study, demonstrating the advantages of surface roughness for fluid flow control. (Marimuthu & Chinnathambi, 2020)

WRLES and WMLES were used to study wake bimodality in the wake flow surrounding a squareback Ahmed Body. The simulations demonstrated how wake dynamics and TKE are produced by front separation bubbles, which is crucial to comprehending wake switching events. (Hesse & Morgans, 2021)

CFD simulations were used to examine the aerodynamic performance of buses in a platoon in crosswind circumstances. The study examined how crosswind affected aerodynamic coefficients and TKE, illustrating how inter-bus distance affects aerodynamic benefits. (Yudianto et al., 2021)

Using ML algorithms as a stand-in for traditional CFD techniques, flow fields across ABR were predicted. When compared to conventional CFD methods, ML-based surrogate models offered significantly more computational efficiency while producing quick and accurate flow field predictions. (Panda & Warrior, 2022)

Using CFD models, the aerodynamic performance of a car with a wind turbine on the back was examined. The study showed a 19.5% drag reduction and assessed the aerodynamic benefits of various control systems. It also examined the impact of plate length on drag reduction. (Feng & Zhang, 2022)

Computational research was done on fluidic on-demand winglets to see if they could lower induced drag on airplane wings. In order to determine the ideal injection settings for reducing drag, the study investigated the effects of injection velocity and angle on aerodynamic coefficients and turbulence characteristics. (Mondal et al., 2023)

To investigate the impact of converging and diverging (C-D) riblets on turbulent flow over an axisymmetric body, DNS were performed. The existence of C-D riblets in the simulations resulted in changes to the aerodynamic forces, turbulence statistics, and flow structures. (H. Wang et al., 2023)

The impact of passive air-blowing on the aerodynamics of an airfoil with a blunt trailing edge was assessed numerically. Using CFD to assess slot design characteristics, the study demonstrated improved aerodynamic performance and decreased turbulence in the wake zone. (Jaffar et al., 2023)

In a nutshell even though the research's methodologies were commendable for tackling turbulent flow phenomena in engineering applications, more improvement and careful assessment are still required. By doing this, researchers can raise the stature and importance of their research, which will ultimately advance our comprehension of turbulent flows and their applicability in real-world scenarios.

2.6 Outcomes

Aerodynamic efficiency, Reynolds number effects, and CL versus angle of attack were assessed using a numerical simulation of an oscillating delta wing. A modest increase in CL at high angles of attack was noted, along with a notable improvement in the lift-to-drag ratio (L/D) throughout a range of Reynolds numbers, in the stall condition and vortex formation. (Hamizi & Khan, 2019)

VIV of a square cylinder was efficiently reduced by slot suction along the leading edge, resulting in up to 92% reduction in vibration amplitudes and 87% suppression of fluctuation lift at optimal suction ratios. At particular suction ratios, TKE peaked, suggesting significant mixing between the near wake and free-end shear flow. (Ying et al., 2019)

On a passenger car, flow management techniques using rear-spoilers and vane-type VG reduced drag by up to 23%, saving up to 11.5% on fuel. The usefulness of rear-spoilers and counter-rotating VG arrays in lowering drag and enhancing flow mixing to prevent separation was demonstrated computationally. (Paul et al., 2019)

A swept wing's riblet drag reduction was simulated using large eddies, which showed nonlinear drag reduction ratios at various sweep angles and maximum reductions of 9.5%. Reynolds stresses were significantly suppressed and turbulence kinetic energy was increased in the wake, according to the study's analysis of local streamline angles, turbulence amounts, and observed laminarization processes.(ZHANG et al., 2020)

In summary, it is crucial to grasp the findings of each study to guide further research efforts toward my topic. Good understanding towards the literature review will lead to a better research produced.

2.7 Turbulent Kinetic Energy (TKE)

For automotive manufacturers to understand and maximize aerodynamic efficiency, TKE is essential. TKE is a measure of the energy attributed to turbulent motion in the airflow surrounding vehicles, which affects the properties of lift and drag. Engineers can find regions of strong turbulence, optimize vehicle designs to reduce energy losses, and improve overall aerodynamic performance for increased fuel efficiency and vehicle stability by analyzing TKE distribution and behaviour.

A key factor influencing flow characteristics is the distribution of TKE caused by dimpled compressor cascades within the boundary layer. Spherical dimples enhance turbulence levels, which in turn reduce separation bubbles on the suction surface and encourage disturbance of the boundary layer. These results emphasize the significance of TKE in improving compressor performance by lowering total pressure loss and mitigating three-dimensional separation close to the hub-corner region (Lu et al., 2019) .

SGS models are evaluated in LES to show that they can accurately predict the behaviour of turbulent flows, including profiles of TKE. The modulation of turbulence and changes in the skin friction coefficient were effectively represented by the SGS models, especially in flows where large-scale vortical structures are caused by geometric disturbances. These results emphasize how crucial SGS models are for modelling turbulent flows with different complexity and boundary conditions (Ramirez-Pastran & Duque-Daza, 2019).

In order to comprehend turbulent energy transfer, an analysis of turbulence over a backward-facing ramp must look at important characteristics such as the dissipation coefficient (Cϵ) and the skewness of the longitudinal velocity gradient (Sk). The study highlights the importance of phase de-coherence processes in non-equilibrium turbulence, an aspect that is sometimes overlooked in turbulence models. It is anticipated that these discoveries will spur additional research into non-equilibrium turbulence processes and improvements in turbulence modeling techniques (Fang et al., 2019) .

Numerous numerical techniques, such as RANS, LES, and DNS, are presented to illustrate the benefits and drawbacks of analysing turbulent flows. LES receives special consideration, with an emphasis on inflow boundary conditions and sub grid size models. The use of turbulence models for particular flow issues in metallurgical processes is also discussed, offering insights into potential future paths for turbulent flow simulation (Y. Wang et al., 2021).

DNS of superhydrophobic drag reduction provides insights into the turbulent kinetic energy TKE budget across various surface configurations. A thorough understanding of the drag reduction mechanism with variable solid fraction and distribution forms of the SHS may be obtained through analysis of TKE formation, dissipation, and diffusion. The study emphasizes how variations in drag reduction affect the Reynolds stress components, highlighting in particular how distribution geometry affects turbulent flow characteristics (Nguyen et al., 2022) .

Research on TKE under a range of flow conditions demonstrates how important it is to comprehend the dynamics of turbulence. Significant changes in TKE and their distribution are revealed through analysis, which might affect flow stability and drag reduction. A thorough understanding of these processes improves turbulence modelling for engineering and aerodynamics applications as well as flow control tactics.

2.8 Drag Reduction

Improving aerodynamic efficiency through drag reduction is a key area of study for the automotive industry in order to improve vehicle performance and fuel economy. The resistance a car experiences while traveling through the air is known as drag, and it has a big impact on both fuel economy and overall performance. In order to reduce drag, one important strategy is to control turbulence in the surrounding airflow.

Airflow patterns produced by turbulence are chaotic and result in increased drag and energy consumption. Thus, techniques to lessen turbulence and optimize the flow field can result in significant gains in aerodynamic performance, which in turn reduces drag and improves fuel efficiency in the design of the vehicle.

The current study used DNS to examine different patterns of SHS on the rotating inner wall in order to evaluate turbulent DR in an incompressible Taylor-Couette flow configuration. The effects of various SHS configurations, such as spiral grooves and streamwise microgrooves, on drag reduction were examined. With streamwise aligned SHS, the largest drag reduction of 34% was attained, demonstrating the efficiency of these surface patterns in altering near-wall dynamics and causing slip at the wall to decrease drag (Naim & Baig, 2019).

There are also method of reducing drag on a passenger car by using a rear spoiler and vane-type VG. Combining VG arrays with a rear spoiler reduces drag coefficient significantly, as shown by experimental and theoretical assessments. Counter-rotating VG arrays are very efficient, reducing drag by approximately 23%. The results show that optimizing the car's aerodynamics with drag reduction strategies can result in fuel savings of up to 11.5%. (Paul et al., 2019)

Porous material affects drag reduction for a van-body truck and can also be uses in wind tunnel testing and numerical simulations as an examination. When porous media is used, aerodynamic parameters such as vortex suppression, surface pressure distribution, and wall shear stress are all improved, leading to a significant decrease in drag. The viability of employing porous media for efficient aerodynamic drag reduction in this application is validated by numerical simulations (Hu et al., 2019) .

Riblet drag reduction effects on an infinite swept wing at low Reynolds numbers using large-eddy simulations are examined. The results reveal non-linear drag reduction ratios across various sweep angles, with a maximum reduction of 9.5% observed at a 45° sweep angle. Analysis of local surface streamline angles and turbulence quantities shows that riblets suppress Reynolds stresses above the wing surface while increasing turbulence kinetic energy in the near wake (ZHANG et al., 2020).

Riblets are a bio-inspired flow alteration technique that reduces drag passively and doesn't need extra power. Using numerical modelling such as FMSSP and CTA, the study investigates riblet effects, concentrating on longitudinal sawtooth-shaped riblets at a maximum Reynolds number (Re) of 1.68 × 105. Up to a 13.2% reduction in shear stress is demonstrated by the results, which also point to an upward shift in the velocity profile close to the wall which lessens drag and turbulence intensity. (Sharma & Dutta, 2023)

Significant reductions in aerodynamic drag are demonstrated by the research conducted on drag reduction processes employing various techniques, including counter-rotating VG arrays, rear spoilers, and VG. Drag coefficients were reduced by adjusting airflow angles, spoiler orientations, and VG configurations. These flow control devices have a practical application for reducing drag and increasing aerodynamic efficiency because they efficiently modify wake topology and decrease TKE.

2.9 Dimple Design

The automotive industry has become interested in dimpled surfaces because of their potential to enhance aerodynamic performance and lessen turbulence. Researchers and engineers are investigating how surface alterations such as those seen on golf balls, which are known to minimize drag, can be advantageous for automobiles. By postponing flow separation and turbulence, dimpled designs modify the properties of airflow, resulting in smoother flow and lower drag.

To maximize aerodynamics, dimple designs are systematically added to vehicle surfaces, such as the hood, roof, or rear, in vehicle applications. Dimples can improve vehicle stability and fuel efficiency by reducing the disruptive effects of turbulence through the manipulation of airflow patterns. In order to improve automotive aerodynamics and lower energy consumption, this research seeks to determine the best dimple layouts for various vehicle shapes and speeds.

An article published in 2019 mentions that the near-bed vortex, which causes scouring, has turbulent energy associated with it that gradually decreases as the scour process progresses. This is especially true for small-scale eddies, which suggests that the dissipated turbulent energy has a role in digging the scour hole (Wei et al., 2019).

While the underbody and wake flow zones are affected by turbulence and slipstream velocity caused by dimple-like cavities beneath the high-speed train. By putting in bogies around these cavities or sealing them off, it is possible to significantly lower slipstream velocity and turbulence, which can result in a 56% reduction in aerodynamic drag and enhance HST performance (J. Wang et al., 2020) .

To improve heat transmission and turbulence characteristics there are studies where spherical cavities on tube surfaces with better heat transfer and a somewhat higher pressure drop, dimpled structures show increased thermal efficiency and the possibility of improved aerothermal performance (Virgilio et al., 2020).

Dimple design provides efficient ways to manage turbulence in the boundary layer and reduce drag, improving aerodynamic efficiency and performance in a variety of applications. These results demonstrate how surface alterations may be advantageous for enhancing flow characteristics and lowering aerodynamic drag.

2.10 Ahmed Body

A widely used model in vehicle aerodynamics for researching turbulence effects and drag reduction is the Ahmed Body. Through the examination of the flow patterns surrounding this simple automotive model, engineers can maximize vehicle configuration to reduce aerodynamic resistance and improve fuel economy. The Ahmed Body is a useful tool for comprehending and enhancing vehicle aerodynamics because of its unique back end and slanting roof, which produce particular flow patterns that affect turbulence and drag. Shown In the Figure 2.3 are the basic dimensions of an Ahmed Body.

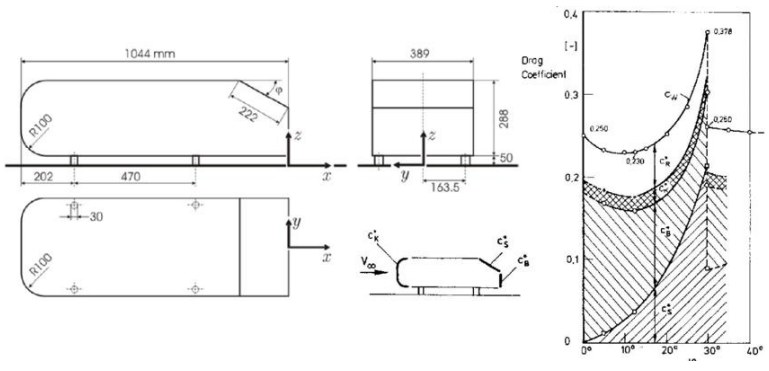

Figure 2.3 Ahmed Body Dimensions (Koppa Shivanna et al., 2021)

An article examines the use of several passive flow controllers to reduce drag on a SBAB model. A variety of cavity configurations are assessed, and it is shown that considerable drag reductions are possible by altering the wake topology as a result of afterbody shape remodelling. This lowers turbulence levels and modifies vorticity patterns (Koppa Shivanna et al., 2021) .

There is also research where the wake behaviour around a 1/4 dimension squareback Ahmed body is studied using LES, with particular attention to turbulence features and bimodal switching. According to the research, huge hairpin vortices that are shed by front separation bubbles aft of the body nose are crucial in producing TKE, which affects wake orientation and bimodal events.(Hesse & Morgans, 2021)

In conclusion, precise design adjustments targeted at lowering drag and managing turbulence within the wake can greatly improve the aerodynamic performance of the Ahmed Body. These results highlight the significance of wake management and form optimization strategies in vehicle aerodynamics.

2.11 Summary

Based on the thorough literature survey described above, it is clear that there is significant continuing study into many elements of turbulent flow dynamics and drag reduction approaches in different fluid systems. Studies have looked into the usage of superhydrophobic surfaces, the effect of particle qualities on turbulent structures, the use of riblets and modified wing shapes to reduce drag, and the analysis of turbulence models and flow characteristics around various geometries.

However, despite a large amount of research done in this field, there seems to be a null in the literature talking about the synergistic effect of TKE and dimple design on bluff bodies for instance the Ahmed Body. While studies have examined drag reduction processes using various approaches, such as surface modifications, riblets, and airflow changes, the combined effect of dimple design and TKE control on bluff bodies like the Ahmed Body has received less attention.

The proposed thesis, "TKE and Dimple Design: Exploring the Synergistic Effect of Drag Reduction on Ahmed Body," seeks to fill this gap by looking into how dimple design, inspired by naturally occurring aerodynamic features, can interact with TKE to improve drag reduction on bluff bodies such as the Ahmed Body. Dimpled surfaces have been found to produce controlled turbulence in the boundary layer, affecting flow characteristics and TKE levels. The research aims to provide insights into how dimple design can successfully influence TKE to generate considerable drag reduction effects by carefully examining the interaction between dimple geometry, turbulence characteristics, and drag coefficients.

The significance of this thesis arises from its potential to help construct more efficient and sustainable transportation systems. With a rising emphasis on reducing fuel consumption and CO2 emissions in transportation, improving aerodynamic efficiency through new drag reduction approaches is essential. By explaining the synergistic impacts of TKE and dimple design on bluff bodies, the study could open the way for the development of next-generation vehicles with better performance and lower environmental impact.

Chapter 3

Methodology

3.1 Introduction

This study uses experimental and computational methods to explore the synergistic effects of dimple design on drag reduction for the Ahmed Body. The methodology is structured to ensure a thorough investigation, starting with creating dimple designs and progressing through detailed CFD simulations and experimental validation. By following a systematic approach, a comprehensive understanding of how different dimple configurations impact aerodynamic performance is aimed to be provided.

The process begins with detailed CAD modelling of Ahmed body featuring various dimple designs (*An_Introduction_to_Computational_Fluid_D*, n.d.). These models are then converted into computational grids and subjected to CFD simulations to analyze airflow characteristics. We validate the quality of our computational meshes and set up appropriate boundary conditions to replicate real-world scenarios accurately (*Fundamentals_of_Aerodynamics*, n.d.). By examining the effects of dimples on boundary layer turbulence and drag reduction, we gain insights into their aerodynamic benefits, supported by both experimental wind tunnel tests and extensive post-processing of simulation data (Menter, 1994)

3.2 Benchmark

In the benchmark stage, a reference point is set to ensure the experimental and computational setups are precise and dependable. The process starts by creating a standard Ahmed Body model and testing it in a wind tunnel to gather baseline data. This data will include key aerodynamic factors like drag coefficient, pressure distribution, and turbulence intensity. By carefully documenting the experimental setup, this ensures the findings are reproducible and provides a solid foundation for comparing the effects of dimple designs.

Simultaneously, a detailed computational model of the baseline Ahmed Body using CFD simulations will be developed. These simulations will replicate the wind tunnel conditions, allowing for a direct comparison with experimental results. Validating the CFD model against experimental data is crucial for confirming its accuracy. This way, trust in the simulations is gained to predict how different dimple designs will affect Ahmed Body, setting a strong base for the rest of the study.

Flowchart Methodology A : Benchmark

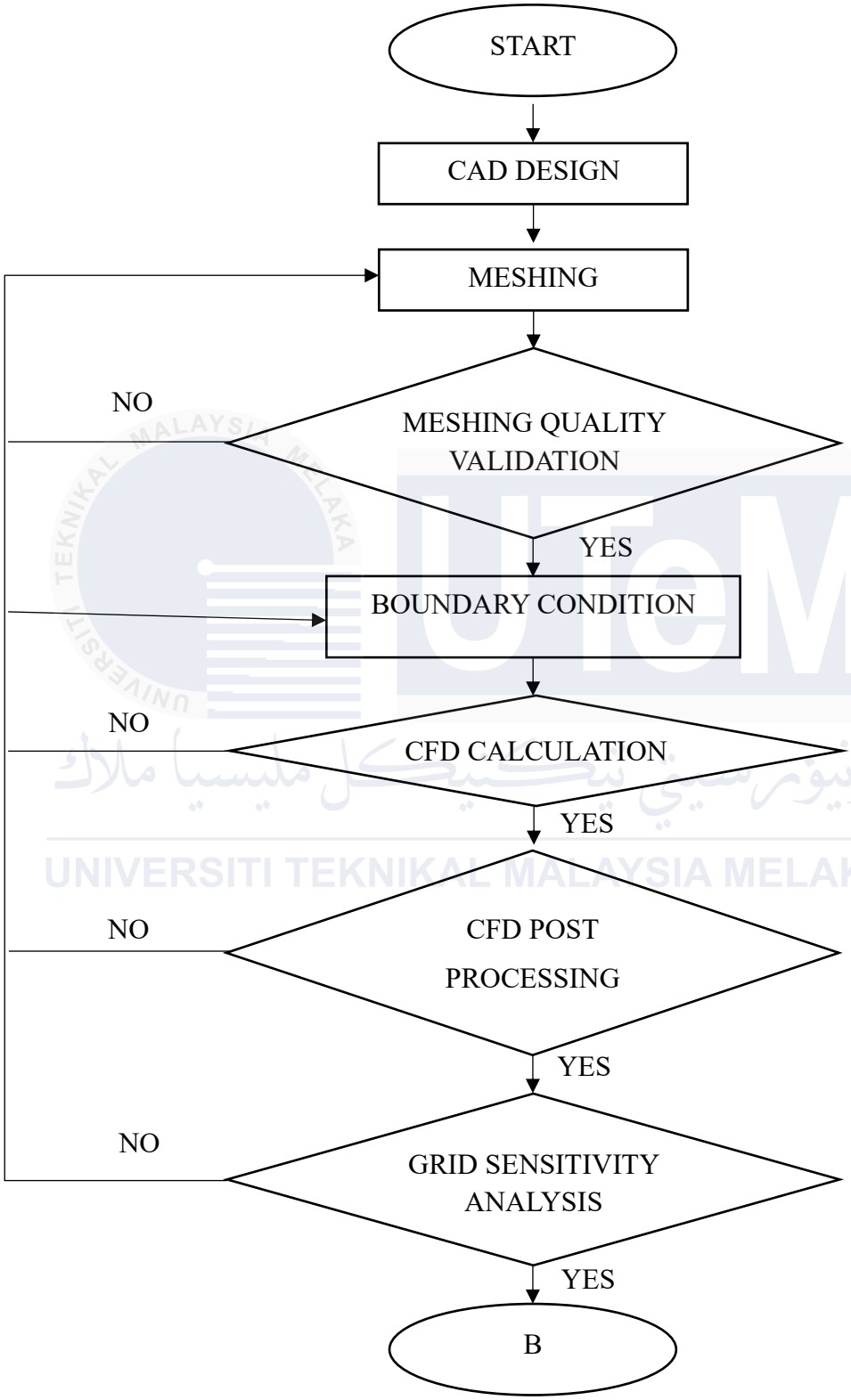

Figure 3.1 Flowchart Benchmark

3.2.1 CAD Design

In the CAD design phase, we create a detailed geometric model of the Ahmed body, serving as the foundation for computational analyses. Using CAD software like SolidWorks or CATIA, we model the standard Ahmed body according to established dimensions and specifications. Then, we modify this model to incorporate various dimple configurations, paying close attention to the size, depth, and placement of the dimples. This design process is iterative, allowing us to adjust based on preliminary findings and theoretical considerations (*An_Introduction_to_Computational_Fluid_D*, n.d.) . Figure 3.2 shows the base page of Catia Software.

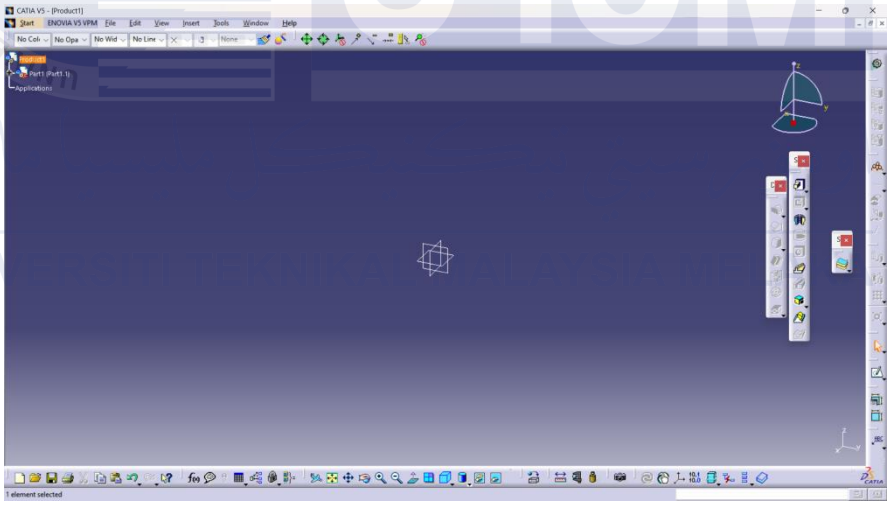

Figure 3.2 Catia Software

Each dimpled design is saved as a separate CAD file, making it easy to compare different configurations. The CAD models are precise to ensure accurate 3D printing for physical testing and seamless import into meshing software for CFD simulations. By maintaining high precision in our CAD models, we can confidently attribute any differences in aerodynamic performance to the dimple designs. This phase ensures all subsequent analyses are based on accurate and consistent geometric representations of the Ahmed body (*Fundamentals_of_Aerodynamics*, n.d.)

The cad design is started with drawing wind tunnel and Ahmed Body design to ensure a stable and balanced testing environment, a symmetrical platform with a width of 2,000 mm was created. A wind tunnel measuring 10,000 mm in length and 4,000 mm in height was designed to provide enough space for aerodynamic testing. An Ahmed body was modeled within the tunnel using standard Ahmed body dimensions, accurately representing a simplified automotive structure for aerodynamic analysis.

To improve the aerodynamic analysis, certain design features were incorporated into the Ahmed Body and the wind tunnel to effectively simulate drag-reducing mechanisms with Ahmed Body components :

i. Carbox Design: A carbox was modelled on the Ahmed body by sketching a rectangle, extruding it to some depth, and renaming as "carbox." In this carbox, it is used as the influence region for meshing and is done with an element size of 15 mm to capture flow separation points around this component effectively.

ii. Underbody Design: In order to capture flow effects underneath the vehicle, an underbody box was also constructed and given an element size of 10 mm for detailed meshing.

iii. Wake Box Design: The area where flow separation and wake creation take place was represented by a wake box that was drawn and extruded onto the Ahmed body. To guarantee accurate data on flow separation and reattachment, this box was meshed with an element size of 10 mm

3.2.2 Meshing

Meshing is a crucial step in CFD simulations, where we divide the CAD model into smaller, discrete elements that the numerical solver uses to approximate the flow equations. Using meshing software like ANSYS Mesher or ICEM CFD, we create a computational grid of the Ahmed body model. The mesh needs to be fine enough to capture detailed flow characteristics, especially in areas with high gradients like the boundary layer, wake region, and around the dimples (*An_Introduction_to_Computational_Fluid_D*, n.d.) A structured mesh or a combination of structured and unstructured meshes will be used to balance accuracy and computational efficiency. Sample of Ansys Software are shown in Figure 3.3.

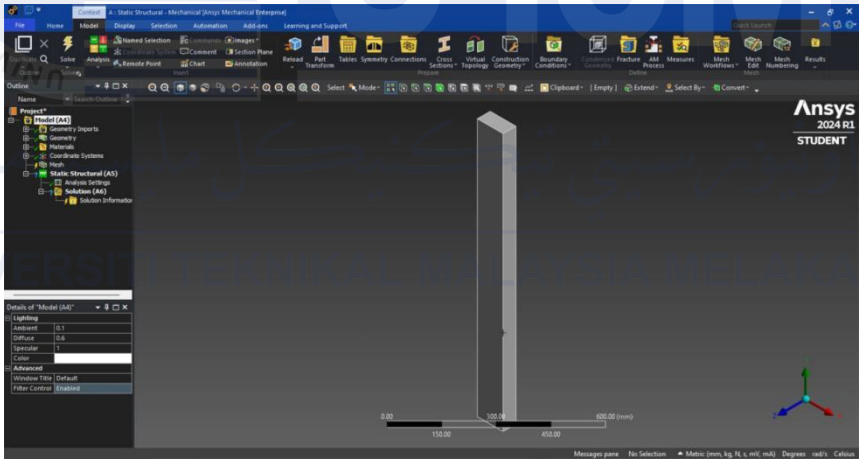

Figure 3.3 Ansys Software

We create finer mesh elements near the surface of the Ahmed body and around the dimples, where detailed flow interactions occur, and coarser elements in less complex flow regions. This approach ensures computational resources are focused where they're most needed. We avoid common meshing issues such as high aspect ratios, skewness, and poor element quality, which can negatively impact the accuracy of CFD results. The goal is to produce a high-quality mesh that accurately represents the physical model while being computationally feasible (Menter, 1994)

3.2.2.1 Wind Tunnel Enclosure Setup

A thorough grasp of actual aerodynamic conditions led to the choice to simulate airflow around the Ahmed body using a box-shaped enclose with uneven cushions. As seen in **Figure, this design successfully simulates the free-stream airflow situation that automobiles encounter.

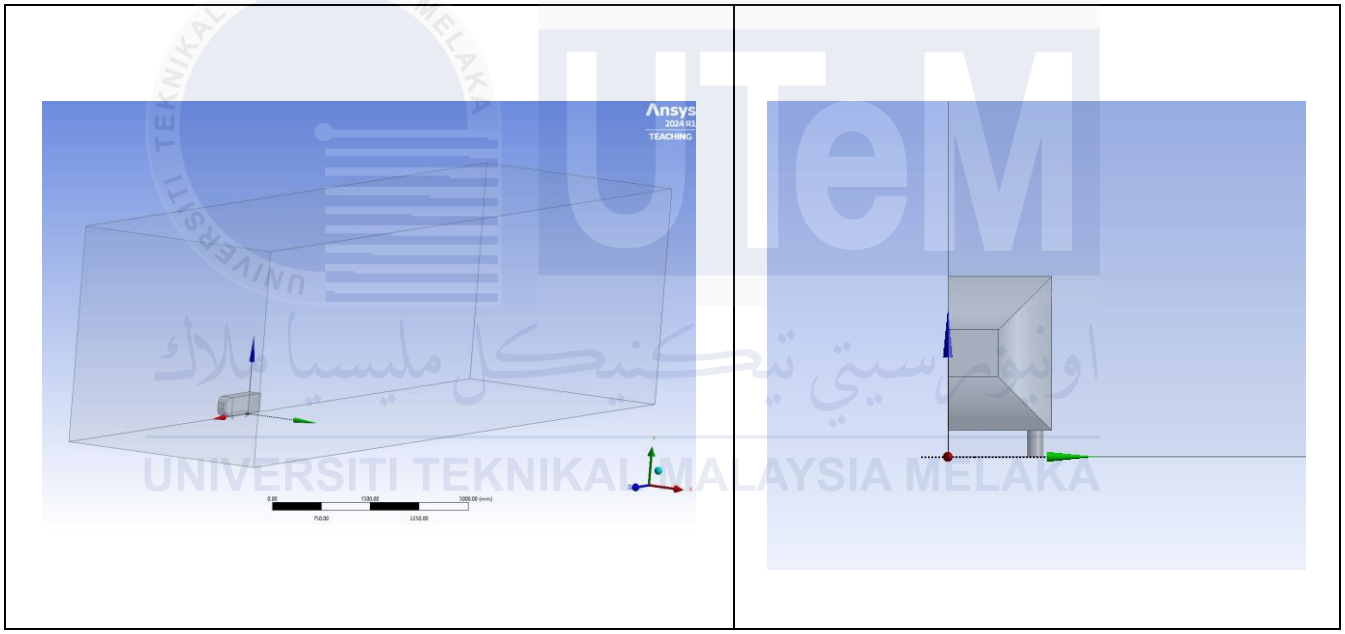

Figure 3.4 Enclosure Position

In places that have significant turbulence, like the wake zone and underbody flow areas, the incorporation of the Boolean subtraction method guarantees the production of a seamless air volume, reducing artificial flow limits and avoiding numerical instabilities. Achieving precise aerodynamic analysis and trustworthy results is greatly aided by these factors.

3.3.2.2. Refinement and Optimization through Meshing

As seen in Figure, advanced meshing techniques were used to improve the simulation's accuracy in important areas, particularly the carbox and wakebox.

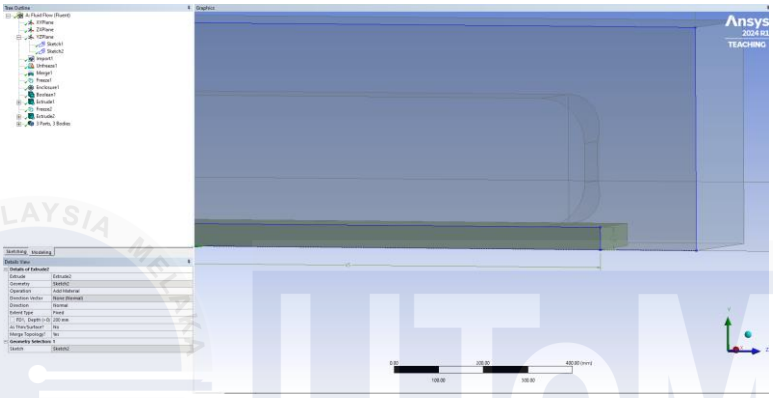

Figure 3.5 Carbox Position

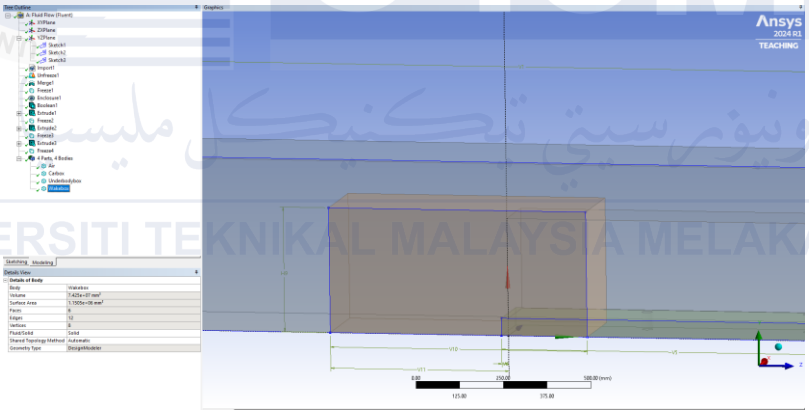

Figure 3.6 Wakebox position

The carbox meshing provides detailed resolution to examine the drag effects caused by design elements, such as in this situation is the dimples, by focusing on capturing flow separation and reattachment locations around the vehicle surface. To capture complex turbulence effects and pressure variations, the wakebox meshing simultaneously targets the wake separation zone. Studies show that when it comes to anticipating intricate flow phenomena, such as small-scale eddies and vortices, a structured mesh with refined sections consistently performs better than a uniformly coarse mesh.

3.2.3 Meshing Quality Validation

Validating the quality of the mesh is essential to ensure our CFD simulations produce reliable and accurate results. The aspect ratio measures the relationship between the lengths of the sides of the mesh elements, with lower ratios generally indicating better quality. Skewness refers to how much an aspect deviates from an ideal shape, such as a perfect square or equilateral triangle, while orthogonality assesses how perpendicular the elements are to each other, affecting the accuracy of gradient calculations (*Fundamentals_of_Aerodynamics*, n.d.)

We use tools within the meshing software to automatically check and refine the mesh, adjusting any elements that don't meet the quality criteria. This step ensures the mesh accurately captures the physical phenomena being studied without introducing numerical errors or artifacts. Additionally, we may conduct sensitivity studies to determine the impact of mesh quality on simulation results, ensuring the mesh provides a good balance between accuracy and computational cost. A high-quality mesh is crucial for obtaining trustworthy CFD results, especially when analyzing complex flow patterns around dimpled surfaces (*An_Introduction_to_Computational_Fluid_D*, n.d.)

3.2.4 CFD Calculation

To evaluate a model's aerodynamic performance, fluid flow is simulated in an organized and systematic manner using the CFD computation technique. The first step in the procedure is model setup, which involves precisely defining the object's shape and the computational domain. Boundary conditions are then applied to as closely mimic the behavior of airflow in the real world as feasible. The input velocity, which indicates the direction and speed of the fluid entering the system, is a crucial component in this configuration. Establishing the prerequisites for a successful fluid dynamics analysis requires this step.

The reference area, which is usually the projected surface area in the direction of flow, is next computed. When calculating aerodynamic forces and coefficients, this region acts as a baseline. Furthermore, to guarantee precise normalization of data, reference values such as velocity, density, and area are established according to the simulation settings.

Convergence requirements are set to preserve numerical stability and accuracy during the simulation. By serving as guiding milestones, these criteria make sure the solver moves steadily in the direction of a trustworthy solution. Performance monitoring is essential to the simulation since it tracks important aerodynamic characteristics. The drag force measures the entire resistance acting on the surface, whereas the Cd quantifies the aerodynamic resistance in relation to the reference area.

Initialization is the last step, in which the solver is given preliminary estimations for the flow variables to enable a seamless and effective convergence process. In addition to ensuring accurate and consistent findings, this methodical procedure offers insightful information about fluid behavior and aerodynamic efficiency. In the end, it is an essential instrument for promoting creativity and efficiency in engineering ideas.

3.2.4.1 Ansys Setup

Determining the geometry and the computational domain is the first step in the ANSYS setup procedure. To do this, a model such as the Ahmed body must be imported or created. Boundary conditions are carefully applied to various areas of the computational domain, such as the inlet, exit, and wall surfaces, after the geometry has been determined. These requirements guarantee that the simulation environment closely resembles the behavior of airflow in the actual world, offering a strong basis for precise results

One of the most essential simulation factors is the inlet velocity. It specifies how much airflow enters the computational domain and in which direction. To duplicate flow circumstances, such a target Reynolds number, this value is usually obtained from experimental data or operating settings. A precise inlet velocity parameter guarantees that the simulation produces accurate results and is in line with actual aerodynamic circumstances.

Table 3.1 Velocity inlet calculation

- Reynolds Number Formula, $\mathrm{Re} = \frac{\rho V L}{\mu}$
- Velocity Formula (derived from Reynolds number) , $V = \frac{\mathrm{Re}\mu}{\rho L}$

$$V = \frac{(1.38\ x\ 10^{6})(1.837\ x\ 10^{-5}\ \frac{Kg}{m}.s)}{(1.225\ kg\ m^{3})(1.044\ m)} = 19.82\ \mathrm{m/s}$$

-
- Temperature and Viscosity μ , 25°C / 298 K | 1.837 X $10^{-5}\ \frac{kg}{m}$.s

The reference area is also established, typically using the anticipated surface area that faces direction of the wind. The Cd and other dimensionless aerodynamic coefficients are calculated using this reference region as a baseline. Other reference parameters, such as velocity, temperature, density, and area, are supplied in addition to the reference area. These numbers are crucial standards for normalizing aerodynamic forces and guaranteeing the significance and comparability of the simulation results.

Next is for the residual setup where convergence criteria are developed in this stage to direct the solution toward accuracy and numerical stability. The numerical imbalance in the governing equations that the CFD solver resolves is measured by residuals. The solver can iteratively improve the solution until it achieves a satisfactory degree of accuracy by clearly setting thresholds for these residuals. In addition to offering insight into the solver's progress, tracking these residuals throughout the simulation process guarantees that the outcomes are dependable and repeatable.

Then definition of the Drag Coefficient Report gave important aerodynamic parameter that gauges the body's aerodynamic resistance in relation to the reference area is the Cd. To determine the drag coefficient based on the forces operating on the surface in the direction of the fluid flow, a report or monitor is set up within the simulation in this stage. When assessing design changes, such the addition of dimples, and how well they reduce aerodynamic drag, this dimensionless number is crucial.

The drag force, in addition to the drag coefficient, is the actual force that the airflow applies on the surface of the model. This force is computed by summing the viscous and pressure forces across the surface of the body. A more thorough understanding of the model's aerodynamic performance and efficiency can be gained by analyzing the drag force in conjunction with the drag coefficient, which provides an absolute assessment of aerodynamic resistance.

By allocating initial estimates for important flow variables including velocity, pressure, and turbulence amounts, the initialization phase gets the computational domain ready for simulation. With a starting point, these initial guesses shorten calculation times and enhance numerical stability. Important aerodynamic parameters like drag force, drag coefficient, and TKE are guaranteed to converge.

Table 3.2 Boundary Condition of Ansys Setup

Boundary Condition	Value
Model k-epsilon	2 Eqn
K - epsilon	Standard
Near – Wall Treatment	Standard Wall Functions
CMu	0.09
C1 - Epsilon	1.44
C2 - Epsilon	1.92
TKE Prandtl Number	1
TDK Prandtl Number	1.3
Velocity Magnitude	19.82
Projection Direction	Z
Min Feature Size [m]	0.001
Area [$\boldsymbol{m^2}$]	0.05756999
Density [kg / $\boldsymbol{m^3}$]	1.225
Length [m]	1.044
Temperature [K]	298.15
Velocity [m/s]	19.82
Viscosity [kg/(ms)]	1.837 $\boldsymbol{e^{-5}}$
Ratio of Specific Heats	1.4
Initialization Z Velocity [m / s]	-19.82
Turbulent Kinetic Energy [$\boldsymbol{m^2/s^2}$]	1.473122
Turbulent Dissipation Rate [$\boldsymbol{m^2/s^3}$]	1337.052

ANSYS simulations generate accurate aerodynamic data by meticulously carrying out these setup steps, offering important insights for performance assessment and design development.

3.2.5 CFD Post-Processing

The last step of analysis in computational fluid dynamics is called CFD post-processing, during which ANSYS Fluent and other tools are used to analyze, interpret, and visualize simulation data. Because it converts unprocessed numerical data into insightful knowledge that informs engineering choices, this stage is essential. To provide a smooth transition into result interpretation, post-processing starts with the importation of simulation data produced during the computational phase.

Velocity contours, pressure distributions, and turbulence characteristics are used to visualize the results using ANSYS Fluent, providing a clear picture of fluid behavior throughout the computational domain. Critical flow processes such fluid separation, vortex formation, and recirculation zones can be identified with the aid of these visual outputs. Such knowledge is essential for assessing aerodynamic performance and comprehending how airflow interacts with the modelled shape.

The next step is quantitative analysis, which focuses on variables like forces, and moments. Mathematical techniques are used to generate these values, which offer exact insights about the fluid's interaction with the object. To verify the precision and dependability of the simulation model, comparative investigations are also carried out, comparing CFD results to experimental data or theoretical predictions.

This procedure not only validates the accuracy of the findings but also enhances comprehension of fundamental aerodynamic concepts. In the end, this phase develops critical thinking, data visualization, and effective simulation output interpretation skills all of which are essential for resolving fluid dynamics engineering problems in the real world.

3.2.6 Grid Sensitivity Analysis

Grid sensitivity analysis, or mesh refinement study, ensures our CFD results are independent of the mesh size and resolution. This involves running simulations with different mesh densities – typically coarse, medium, and fine meshes. The goal is to see if the simulation results, like drag coefficient and pressure distribution, stay consistent as the mesh gets finer. If the results change significantly with mesh size, it means the mesh isn't fine enough to capture the necessary flow details (*Fundamentals_of_Aerodynamics*, n.d.)

We start by generating a series of meshes with varying densities and running simulations for each one. Then, we compare the results to evaluate how sensitive key output parameters are to the mesh size. By plotting these parameters against the number of mesh elements or grid spacing, we can identify when further refinement doesn't significantly change the results, indicating grid independence. This step is crucial for ensuring the accuracy and reliability of our CFD results, confirming that the mesh resolution is adequate to capture the physical phenomena without introducing errors due to insufficient discretization (*An_Introduction_to_Computational_Fluid_D*, n.d.). Figure 3.4 shows example of grid sensitivity analysis.

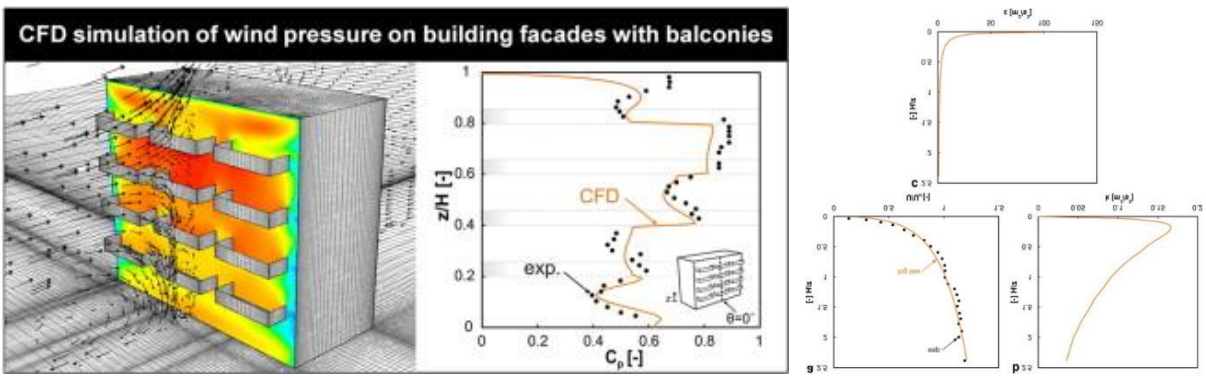

Figure 3.7 Example of Grid Sensitivity Analysis (Montazeri & Blocken, 2013)

3.3 Validation Process

Making sure the research is rock solid is super important, this validation process got in place. It's like a step-by-step journey where it starts by playing around with different dimple designs and end up analyzing tons of data to see how they affect the Ahmed Body aerodynamics. Imagine it like building a puzzle, each piece fitting perfectly into the next.

First up, creativity with CAD software is explore, and all sorts of design dimple configurations. Then, it is moves to technical part, turning those designs into computational grids for simulations. From there need to be sure the grids are top-notch, things are check like shape and size to ensure accuracy. Once the grids are ready, it's time to set everything up.

Then, simulations are started, seeing how air flows around the Ahmed Body with different dimple setups. Proceed for the results, looking at how turbulence is affected and how much drag gets reduced. Once all the numbers are gained, the data is visualized to make sense of it all and dig into what it all means for dimple designs and drag reduction.

Flowchart Methodology B : Modelling

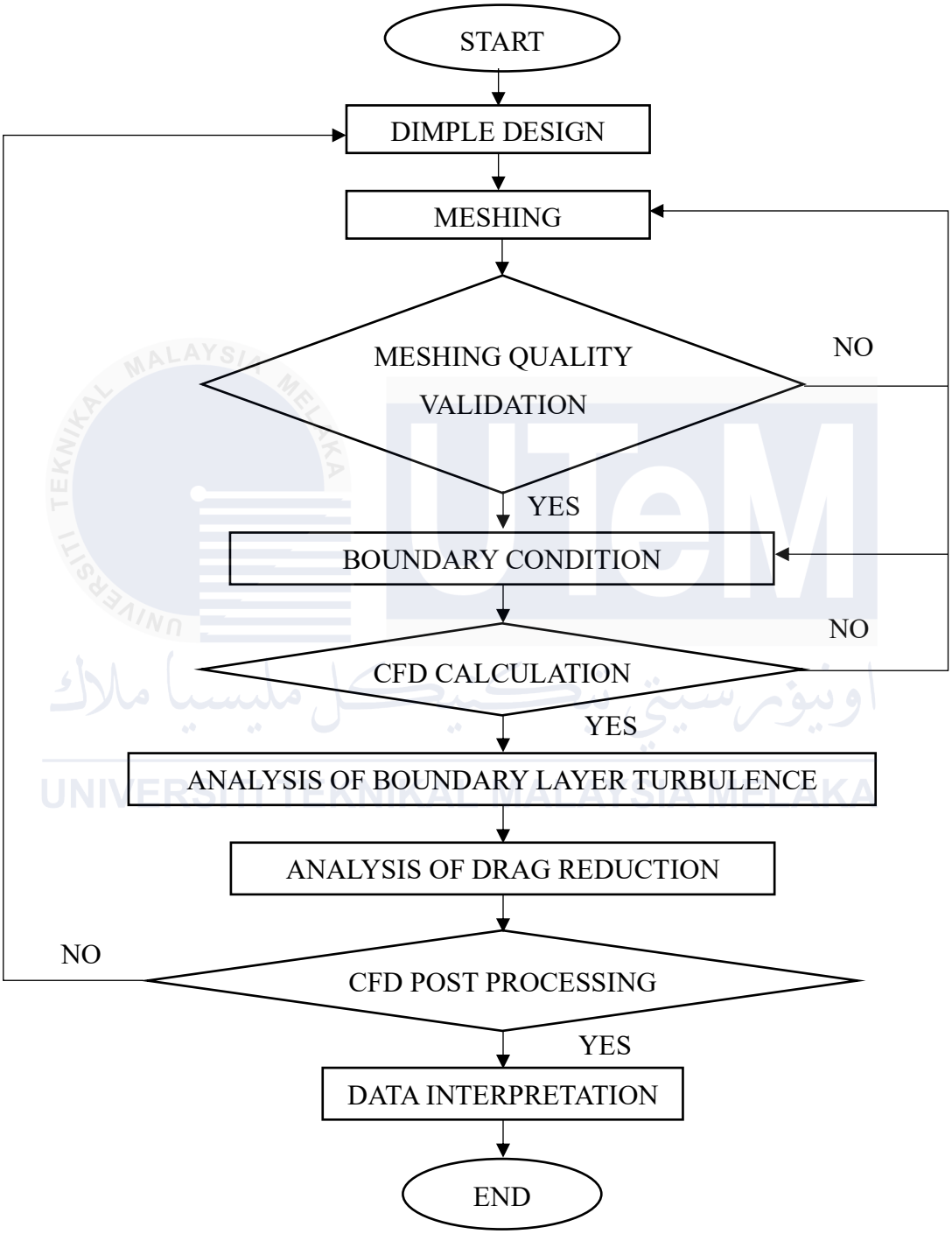

Figure 3.8 Flowchart of Validation Process

3.3.1 Dimple Design

The design are informed by theoretical research and previous studies that suggest specific dimple configurations might be effective in altering the flow characteristics around the Ahmed body. Each design aims to manipulate the boundary layer and turbulent structures to achieve a reduction in aerodynamic drag.

Once the CAD models are complete, they are prepared for CFD simulations. For computational analysis, the models are imported into meshing software to create detailed computational grids (Ferziger & Peric, n.d.). This phase not only provides a foundation for understanding how dimples affect drag but also guides the selection of the most promising designs for further analysis (Menter, 1994)

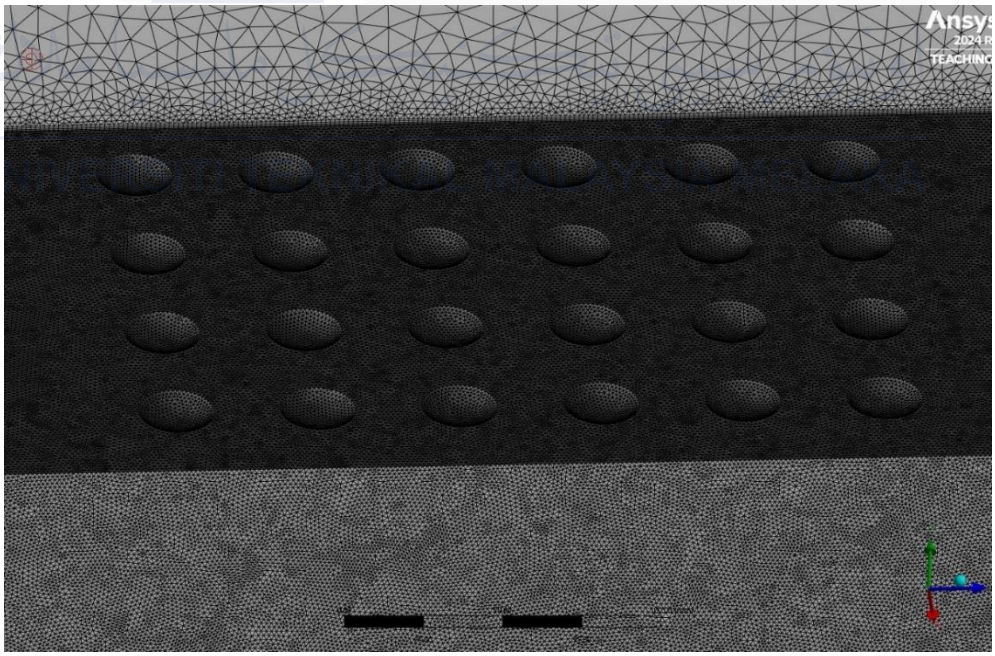

Figure 3.9 Dimple Setup in Catia

3.3.2 Analysis of Boundary Layer Turbulence

The analysis of boundary layer turbulence plays a critical role in understanding how dimple augmentation affects the aerodynamic performance of an Ahmed Body. ANSYS Fluent, an effective CFD program renowned for its accuracy in simulating turbulent flows, is used to conduct this inquiry.

The thin area close to a body's surface where fluid velocity drastically shifts from zero (at the wall) to the free stream velocity is known as the boundary layer. Since this area directly affects flow separation and aerodynamic drag, accurate study is crucial.

The first step is to import the dimple-augmented Ahmed Body's geometrical model into ANSYS Fluent. To capture the features of the dimples and their impact on the boundary layer, the mesh which was initially produced in CATIA is further improved.

Because standard models like k-ε and k-ω are good at capturing extremely turbulent flow behavior close to the surface, they are usually used for turbulence modelling. To guarantee that the simulation faithfully mimics actual conditions, suitable boundary conditions are established at the inlet, outflow, and walls.

ANSYS Fluent solves for important fluid properties in the boundary layer throughout the simulation, such as velocity, pressure, and turbulence intensity. The information produced sheds light on the dynamics of vortex generation, the sites at which laminar and turbulent flow transition, and the role dimples play in these processes.

The effectiveness of dimples in delaying flow separation, lowering drag, and improving aerodynamic efficiency is determined by this analysis. Dimple shapes are optimized for improved aerodynamic performance by carefully examining parameters like the skin friction coefficient and TKE.

3.3.3 Analysis of Drag Reduction

The analysis of drag reduction is the central focus of our study, aiming to quantify the impact of various dimple designs on the aerodynamic performance of the Ahmed Body. In the experimental setup, we conduct wind tunnel tests to measure the drag forces acting on both the baseline and dimpled models (Barlow et al., 1999). Force sensors are used to capture precise drag measurements, while pressure sensors provide detailed data on pressure distribution across the surface of the Ahmed Body.

In addition to experimental measurements, CFD simulations offer a comprehensive breakdown of the drag forces acting on the Ahmed Body (*An_Introduction_to_Computational_Fluid_D*, n.d.). By separating pressure drag and friction drag, we can understand how dimples influence different components of the total (SPALART & ALLMARAS, 1992). The simulations also provide detailed flow visualizations, showing how dimples alter the wake structures and flow separation points (BALACHANDAR et al., 1997). This analysis not only confirms the potential of dimples for improving aerodynamic efficiency but also provides valuable insights for future design improvements in automotive and aerospace applications (Stephen B Pope, 2001). Figure 3.7 shows the schematic diagram of the interaction between the grooved surface and streamwise vortex.

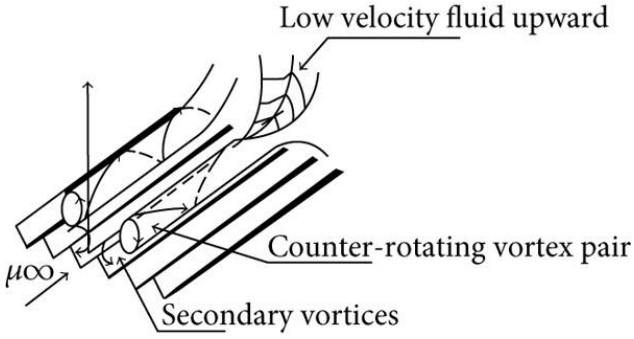

Figure 4.10 Schematic diagram of the interaction between the grooved surface and streamwise vortex. (Yunqing et al., 2017)

3.3.4 Data Interpretation

Understanding the aerodynamic behavior of a dimple-augmented Ahmed Body, especially with regard to the Cp and Cd, requires the interpretation of CFD data.

Drag forces are mostly determined by the distribution of pressure. High and low-pressure zones can be recognized using pressure contour plots, particularly at the Ahmed Body's rear end where low-pressure zones greatly increase aerodynamic drag. Dimples can encourage the creation of advantageous pressure gradients by changing airflow patterns, which aids in lowering drag.

Comparing pressure gradients across various bodily locations is made simpler by the Cp, which normalizes pressure data. This research identifies regions where dimples improve airflow homogeneity and reduce pressure drag by mitigating adverse pressure gradients.

Conversely, the Cd measures the resistance that the Ahmed Body encounters about the reference area and dynamic pressure. Because less energy is lost overcoming airflow resistance, a lower drag coefficient denotes increased aerodynamic efficiency.

Dimples help reduce drag by boosting turbulence mixing, which dismantles big, drag-inducing vortices, decreasing wake regions, and postponing flow separation. Better aerodynamic performance and reduced drag forces are the results of these factors taken together.

The aerodynamic modifications brought about by the dimple design are revealed by a thorough examination of the velocity and pressure fields surrounding the Ahmed Body. This information demonstrates whether the changes were effective in lowering drag without sacrificing stability.

3.4 Summary

This chapter examines the impact of dimple designs on bluff body drag reduction, with a particular emphasis on the Ahmed Body. It starts by stating the goals of the study and the significance of modifying dimples to increase aerodynamic efficiency.

The process's essential steps includes CAD design, meshing, CFD computing, post-processing, and grid sensitivity analysis that are covered in order to guarantee accurate and trustworthy simulations. The importance of boundary conditions in simulating real-world flow behavior is also emphasized in this chapter.

Using models such as k-ε and k-ω, the analysis explores boundary layer turbulence, emphasizing the role dimples play in flow separation, vortex production, and overall aerodynamic efficiency. The efficiency of dimple designs in lowering drag forces is also assessed using metrics like the Cp and Cd.

In summary, this chapter offers a methodical way to investigate the aerodynamic effects of dimples, providing information on how they could improve performance and laying the groundwork for additional research and improvement in subsequent sections.

Chapter 4

Result

4.1 Introduction

In this chapter, it present the results of experimental and computational analyses on how dimple designs affect drag reduction on Ahmed Body. This focus on key factors like the drag coefficient (Cd), flow separation, and the distribution of turbulent kinetic energy (TKE) to show improvements in aerodynamic performance.

The results, derived from CFD simulations, ensure accuracy and reliability. Then it is compare to dimple-modified design with the standard Ahmed Body model to illustrate how these surface changes influence boundary layer behavior and airflow patterns.

By examining pressure distribution, velocity, and TKE, we explain the relationship between dimple shape and aerodynamic efficiency. We explore how dimple-induced turbulence delays flow separation and reduc overall drag.

This chapter aims to clearly and systematically present these findings to provide insights into how dimples can enhance aerodynamic efficiency. These results will serve as a foundation for the next chapter, where we will discuss implications and potential improvements.

4.2 Grid Sensitivity Analysis

Grid sensitivity analysis is essential to ensure the accuracy and reliability of simulation results in CFD. It involves evaluating the effects of grid resolution variations on important aerodynamic characteristics such as pressure distribution, drag coefficient, and velocity profiles. This procedure assists in determining the ideal grid density that strikes a balance between computational cost and result accuracy by methodically improving the grid and examining the alterations in the data that follow.

Grid sensitivity analysis aims to reduce numerical mistakes brought on by insufficient grid resolution and ensure that grid dependence has no impact on the outcomes. A well-fine-tuned grid captures essential flow properties, particularly in high-gradient areas like wake and separation zones. This section examines the grid sensitivity study's findings, including information on the selected grid resolution and how it affects the Ahmed Body's overall aerodynamic analysis with dimple adjustments.

4.2.1 Pressure Coefficient (Cp)

The distribution of pressure across a body's surface in a fluid flow is defined by the dimensionless Cp. It is crucial for locating places that are sensitive to flow separation, aerodynamic drag, and high and low pressure.

This section assesses the effect of grid density on pressure prediction accuracy by analyzing the distribution of Cp across various grid resolutions. Cp values steady with increasing grid size, suggesting that the outcomes are not affected by grid resolution.

Without being impacted by grid size, this stability guarantees precise pressure distribution. Cp values, for example, are greater and less refined when the grid has 3 million elements, indicating that the grid is too coarse to record fine-grained pressure fluctuations. Cp values stabilize at a grid size of 9 million elements, providing a suitable trade-off between computational cost and accuracy. Grid independence is confirmed by the modest changes in Cp that result from further refining to 12 and 15 million components.

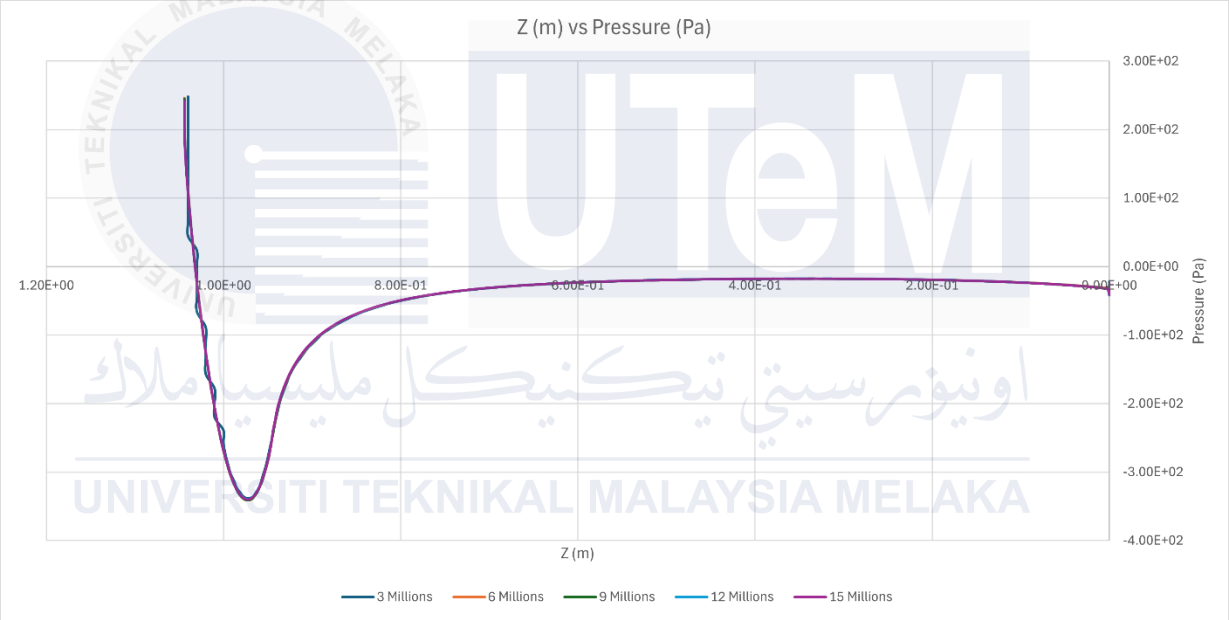

Figure 5.1 Pressure Coefficient of Benchmark Element Value

Figure 4.1 explores the effects of dimple adjustments on pressure distribution through a thorough investigation of the Cp contour and profile. The link between surface geometry and aerodynamic performance is better-understood thanks to these insights, which also emphasize the significance of selecting the appropriate grid resolution for accurate simulation results and the role that pressure behavior plays in reducing drag.

Accurate assessments of aerodynamic performance, including drag and lift forces, depend on the correct capture of the pressure distribution, which is demonstrated by stable Cp values across different grid sizes. Finding areas of high and low pressure is aided by the Cp graph, which normally shows peaks and valleys. These characteristics are essential for locating regions with high aerodynamic loads and possible flow separation. Overall, the Cp graph analysis indicates that the best balance between precision and computing efficiency is achieved with a grid size of 9 - 12 million elements.

4.2.2 Benchmark Grid Sensitivity Analysis

Cd for different grid sizes in the CFD simulation are compared in Table 4.1 The following drag coefficient values are displayed in the results, for 3 million, 6 million, 9 million, 12 million, and 15 million elements. 3 million elements have a value of 0.3164, 6 million have a value of 0.3077, 9 million have a value of 0.3070, 12 million have a value of 0.30651, and 15 million have a value of 0.3041. The drag coefficient falls with increasing grid size, suggesting that finer grids better predict drag and capture more intricate flow features. Drag is significantly reduced between 3 million and 6 million elements, indicating that grid resolution first significantly impacts accuracy. Once 9 million elements are reached, the drag coefficient values converge from 0.3070 to 0.30651 accuracy, becoming almost constant.

Table 4.1 Comparison of Drag Coefficient with Meshing Size

No.of Element	Mesh Value	Drag Coeff
3 Million	0.0038	0.3164
6 Million	0.00232	0.3077
9 Million	0.0017	0.3070
12 Million	0.00144	0.30651
15 Million	0.00128	0.3041

For dependable findings, a grid size of 9 – 12 million elements is ideal. Minor numerical errors or particular simulation parameters may be the cause of the drag coefficient's modest rise at 15 million elements (0.3041) as opposed to 12 million elements (0.3065). But because this change is so tiny, it does not affect the overall trend or conclusion.

According to this investigation, a grid size between 9 and 12 million elements provides the best choices between computing performance and accuracy. With notable gains seen up to 9 million elements, the results highlight how sensitive CFD simulations are to grid size. The drag coefficient stabilizes after this, suggesting grid independence and little improvement with additional tuning. This analysis demonstrates that a grid size of 9 to 12 million elements provides accurate aerodynamic predictions while preserving computational efficiency.

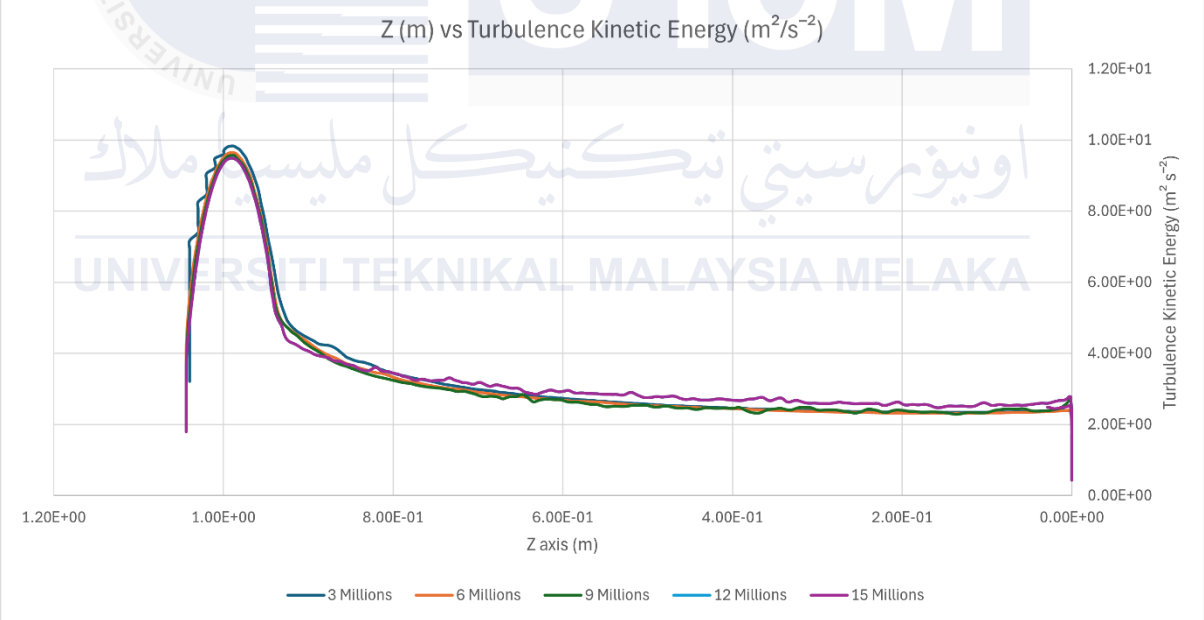

Figure 4.2 TKE *of Benchmark Element*

TKE variability across grid resolutions is shown in Figure 4.2, which adds light on how different degrees of detail are used to record turbulence properties. The findings demonstrate that TKE values rise as grid sizes go finer, suggesting that more complex and smaller turbulent structures are captured by increased grid resolution.

The TKE values, for example, are significantly less at 3 million elements, demonstrating that a coarse grid cannot resolve finer turbulence characteristics. The TKE values keep rising as the grid size grows to 6 and 9 million elements, indicating a better capacity to record turbulence structures. The TKE values increase and stabilize at 12 million elements, indicating that this grid size is adequate to resolve most turbulence features efficiently. The TKE values show little change beyond this, at 15 million elements, suggesting that there is little additional benefit to further refinement.

Finding the places with the highest turbulence made it easier by the distribution of TKE over various planes, which also offers important information about flow behaviour, such as possible sites of flow separation or attachment. Grid independence is confirmed by the stabilization of TKE values with increasing grid size, indicating that the simulation faithfully captures turbulence behaviour without the need for extra grid refinement.

In conclusion, the analysis highlights how crucial sufficient grid resolution is to precisely capture turbulence properties. The optimal balance between preserving computational efficiency and capturing intricate turbulence structures is found to be a grid size of 12 million elements.

4.3 Comparison of Benchmark Design and Dimple Design

The Dimple Design and the Benchmark Design are two distinct designs which aerodynamic efficiency is compared in this study. To assess their aerodynamic performance, the analysis focuses on important metrics such as the drag coefficient, TKE, velocity contours, and pressure distribution.

While TKE offers important information about the energy contained in turbulent eddies in the airflow, the drag coefficient is the main measure of aerodynamic efficiency. By highlighting regions of even or irregular airflow, velocity contours aid in the visualization of the flow patterns surrounding the designs. In the meantime, areas of high and low pressure are identified by analyzing the pressure distribution using total pressure contours across several planes.

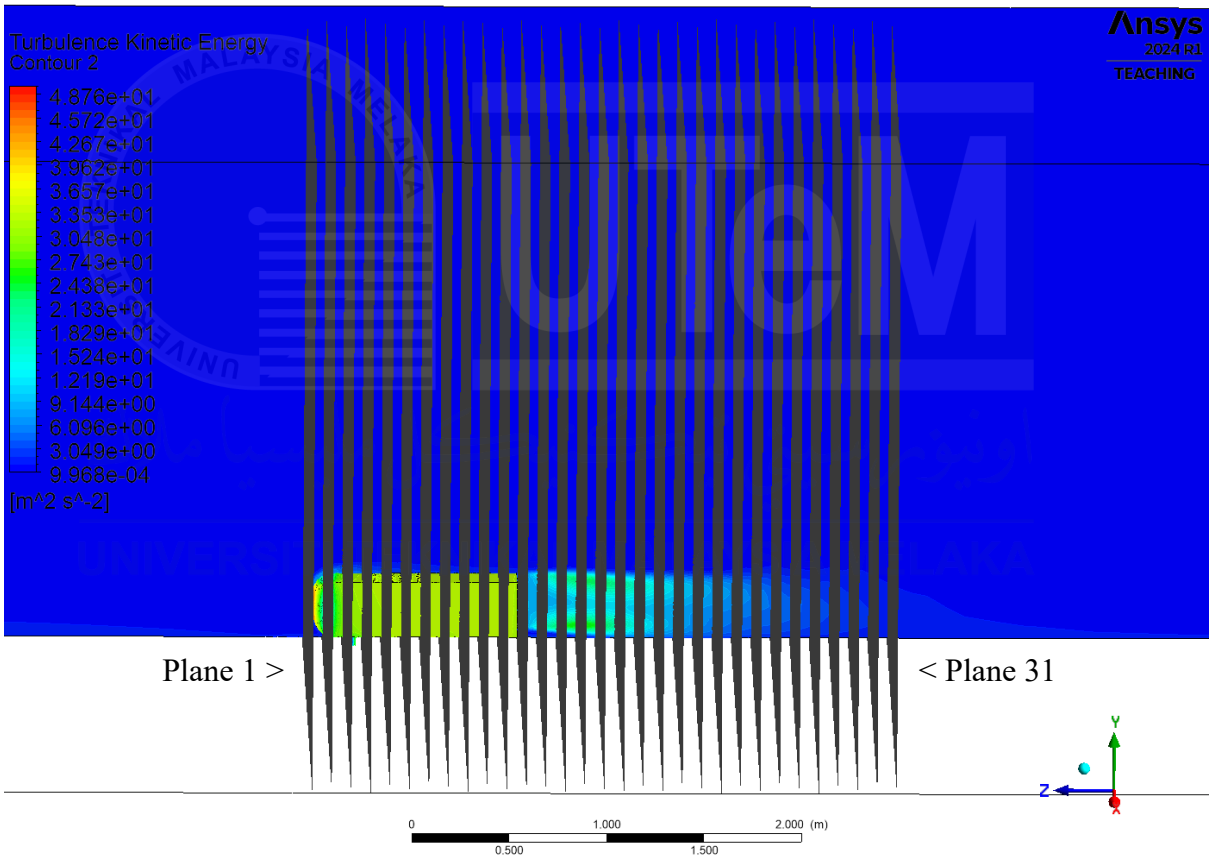

Figure 4.3 Plane throughout Ahmed Body

This study intends to identify possible methods for enhancing overall performance by examining these factors to draw attention to the variations in aerodynamic behavior between the two designs.

4.3.1 Drag Coefficient

The Cd of the Benchmark Design and the Dimple Design are compared in Table 4.2. Drag, which is measured by the drag coefficient, is the resistance an item experiences when moving through a fluid. Better aerodynamic efficiency is usually indicated by a lower Cd value in aerodynamics.

Table 4.2 Difference of Ahmed Body Benchmark & Dimple Design

	Benchmark	Dimple Design
Drag Coeffcient	0.30651	0.2784

To evaluate the aerodynamic performance of both designs, this study compares and analyzes their drag coefficients under the same circumstances. According to the data, the Dimple Design attains a reduced drag coefficient of 0.2784, whereas the Benchmark Design has a drag coefficient of 0.3065. This discrepancy implies that the Dimple Design improves aerodynamic efficiency by producing less drag.

These results demonstrate how dimples can improve performance and show how useful it is to include them in the design. This comparison offers important information on how aerodynamic behavior might be optimized by surface adjustments.

4.3.2 Velocity Separation

The benchmark design and the dimple design have significantly different aerodynamic efficiencies, according to the separation zone and separation velocity calculations. TKE contours and pressure coefficient are used to analyze the separation zone, which is where airflow separates from the surface.

The benchmark design has bigger separation zones, which are defined by wide areas of low pressure and high turbulence levels, as shown in Figure 4.4. The Dimple Design, on the other hand, has notably smaller separation zones, greater pressure values, and less turbulence intensity. This suggests that the Dimple Design has less flow separation and more steady airflow.

Improved aerodynamic efficiency corresponds closely with the Dimple Design decreased separation areas, underscoring the usefulness of surface dimples in regulating airflow and reducing drag.

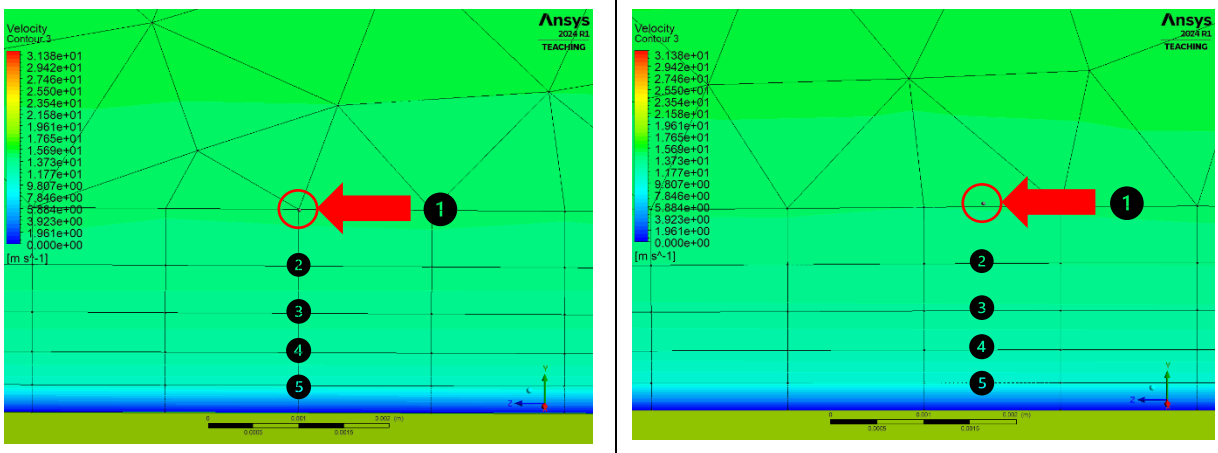

Figure 4.4 Comparison Separation Velocity on Same Scope Position

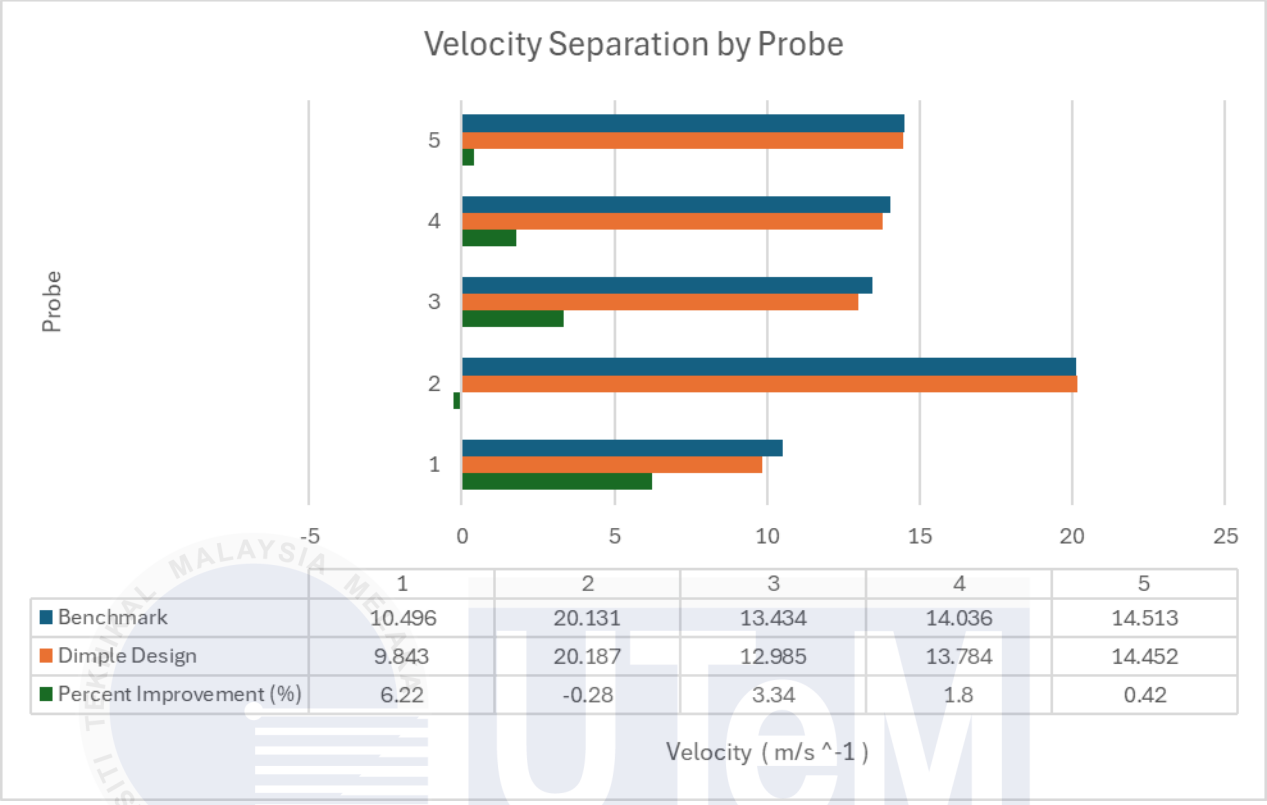

	1	2	3	4	5
Benchmark	10.496	20.131	13.434	14.036	14.513
Dimple Design	9.843	20.187	12.985	13.784	14.452
Percent Improvement (%)	6.22	-0.28	3.34	1.8	0.42

Figure 4.5 Difference Separation Value on 5 Same Scope Position

As shown in Figure 4.5, velocity contours are used to analyze the velocity separation effects by displaying flow behavior and fluctuations inside the separation zone using a probe. Significant velocity changes are seen in the Benchmark Design close to the separation region, suggesting unstable and disturbed airflow, which raises drag. On the other hand, a more stable and regular airflow pattern is produced by the Dimple Design's smoother velocity contours and much lower velocity separation.

The results in Figure 4.5 demonstrate how the Dimple Design increased flow uniformity successfully reduces drag and increases aerodynamic efficiency.

All things considered, the Dimple Design improves the Benchmark Design in terms of aerodynamic reliability and efficiency by reducing the amount of separation and velocity fluctuations.

4.3.3 Velocity Distribution

Designing anything that is stable and aerodynamically efficient requires an understanding of how velocity changes within a flow field. A wake and increased drag can result from the airflow separating from the surface due to abrupt changes in velocity. Conversely, smoother velocity distributions lower drag and increase efficiency by keeping the airflow affixed to the surface.

As seen in Figure 4.6, a balanced velocity field also results in a more uniform pressure distribution, which is essential for preserving stability and reliable performance.

Velocity	
Benchmark	Dimple Design
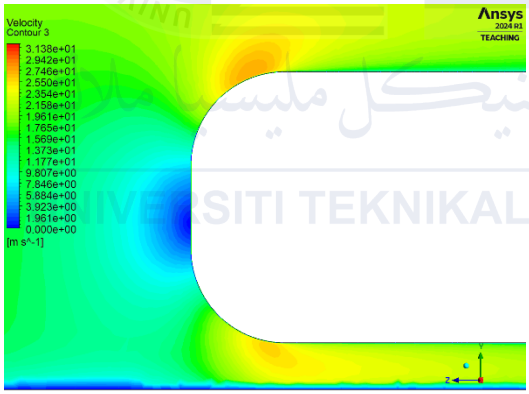 Side View of Ahmed Body	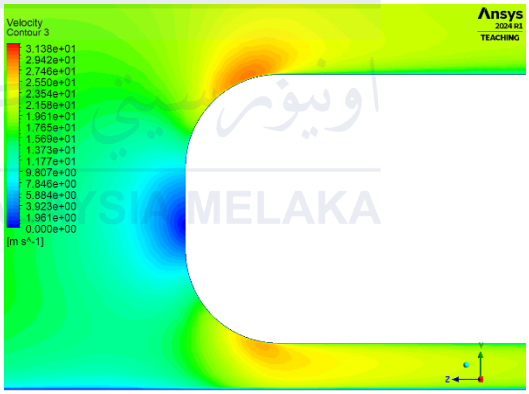 Side View of Ahmed Body
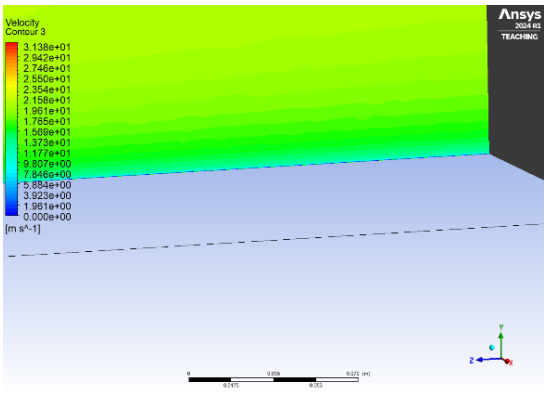 Close Up View of Before Dimple Position	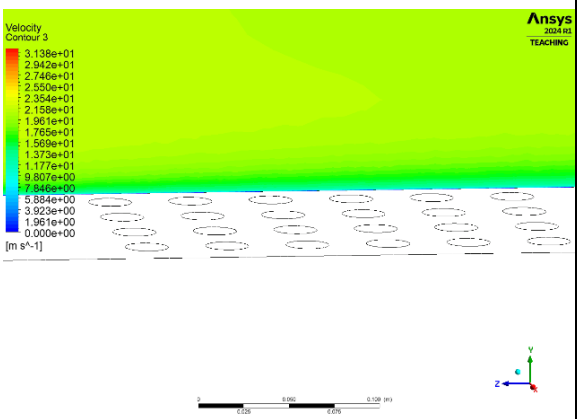 Close Up View of Dimple Position

Figure 4.6 Comparison of Velocity Plane Distribution

Figure 4.6 illustrates the impact of turbulence levels on the velocity profile. High variations in velocity frequently increase turbulence, wasting energy and decreasing efficiency. Reduced turbulence from smoother velocity profiles improves flow efficiency and saves energy. This is due to the fact that a design's drag and lift forces are directly impacted by the distribution of velocity.

Although they don't substantially alter the overall velocity distribution, dimples can enhance aerodynamics. They primarily impact the wake zone behind the item and the boundary layer near the surface. Dimples in the boundary layer smooth the airflow, lowering turbulence and local flow separation. They aid in enhancing velocity recovery in the wake region. These impacts are modest, though, and the airflow that is farther away from the surface is largely unaffected.

For steady and effective aerodynamic performance, velocity distribution throughout the flow field must be controlled. Although dimples aid in wake recovery and boundary-layer flow smoothing, their overall influence on large-scale velocity patterns is minimal.

Where airflow increases or decreases is indicated by the velocity distribution. According to Bernoulli's principle, high-velocity regions, which are frequently produced by streamlined surfaces or restricted flow channels and correspond to reduced pressure, which aids in the creation of lift. Low-velocity regions, typically located in flow separation or recirculation zones, have higher pressure and may result in flow instability, which can compromise stability and aerodynamic efficiency.

4.3.4 Pressure Distribution

Pressure distribution directly influences lift and drag forces, it is essential to a design's aerodynamic efficiency. The Cp contours, which illustrate how pressure changes throughout the design, are displayed in Figure 4.7. Lower Cp values, which are frequently associated with possible flow separation, suggest low-pressure zones, whereas higher values indicate high-pressure locations.

The benchmark design uneven pressure distribution increases drag and may cause flow instability. The Dimple Design, on the other hand, provides a more consistent and steady pressure distribution, which reduces drag and improves aerodynamic performance. Better pressure recovery and less flow separation are indicated by the higher Cp values in the Dimple Design, which enhance flow efficiency and stability.

Pressure Coefficient	
Benchmark	Dimple Design
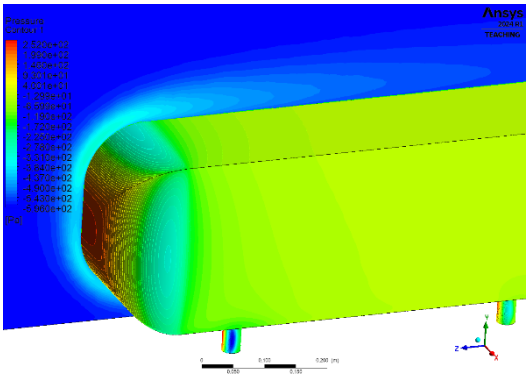	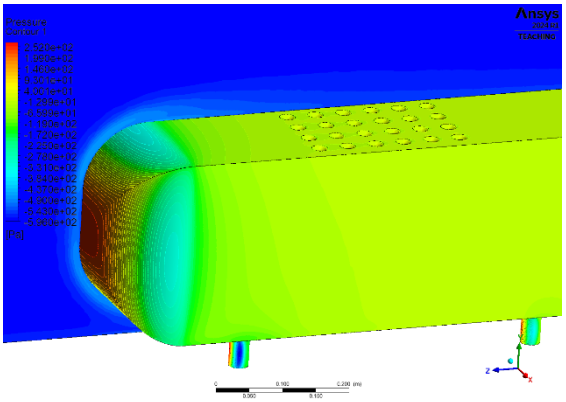
Isometric View of Ahmed Body	Isometric View of Ahmed Body

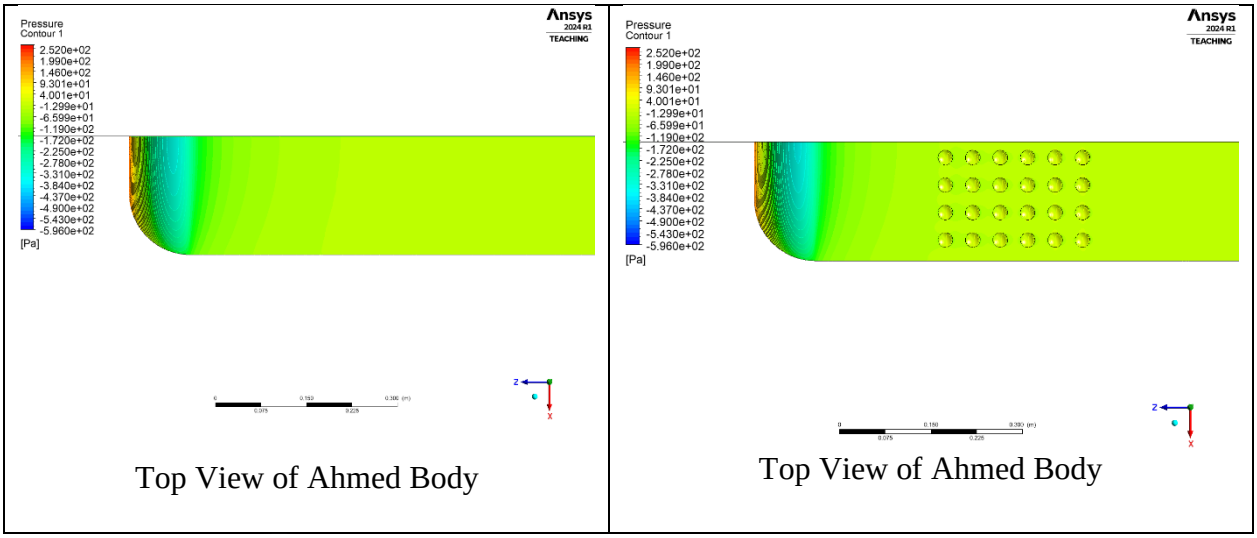

Figure 4.7 Comparison of Pressure Contour

However, the Ahmed Body surface and wake zone are the only areas where dimples have a significant effect on pressure distribution. Although dimples lessen flow separation and assist in maintaining the flow linked, they have little effect on the total pressure distribution. Regions, such as the low-pressure wake zone, where dimples lessen turbulence and provide a more seamless pressure recovery, see the most gains.

Sustaining good performance and aerodynamic stability requires a balanced pressure field. Unmanaged low-pressure zones can create drag and interfere with smooth airflow, whereas high-pressure areas aid in creating lift. Dimples and other surface characteristics are frequently employed to produce a more evenly distributed pressure, which lowers drag and boosts overall efficiency.

4.4 Turbulence Kinetic Energy

TKE analysis shows how turbulence dynamics, linked with the Bernoulli Principle, can maximize aerodynamic performance. According to the Bernoulli Principle, as a fluid's velocity increases, its pressure falls. The dimples on the Ahmed Body contribute to this by lowering energy loss in the flow, leading in a lower TKE and a more stable velocity distribution, which results in a smoother flow pattern.

This stabilization has a direct impact on surface pressure distribution: quicker and more streamlined flow reduces high-pressure zones associated with flow separation and recirculation. Drag forces are minimized as velocity and pressure gradients align more efficiently, resulting in increased aerodynamic efficiency. Furthermore, the dimples assist manage turbulent energy, allowing for smoother flow reattachment and decreasing pressure variations throughout the body.

The combined result of minimizing TKE and aligning with Bernoulli's velocity-pressure relationship demonstrates the dimple design's ability to greatly reduce drag and improve overall flow dynamics.

4.4.1 Mean, Median and Standard Deviation

In the context of Turbulence Kinetic Energy (TKE), this section compares the energy levels for two designs: Benchmark and Dimple Design. TKE, a measurement of the energy contained in a fluid's turbulent motion, is essential for comprehending and improving fluid dynamics in a variety of engineering applications.

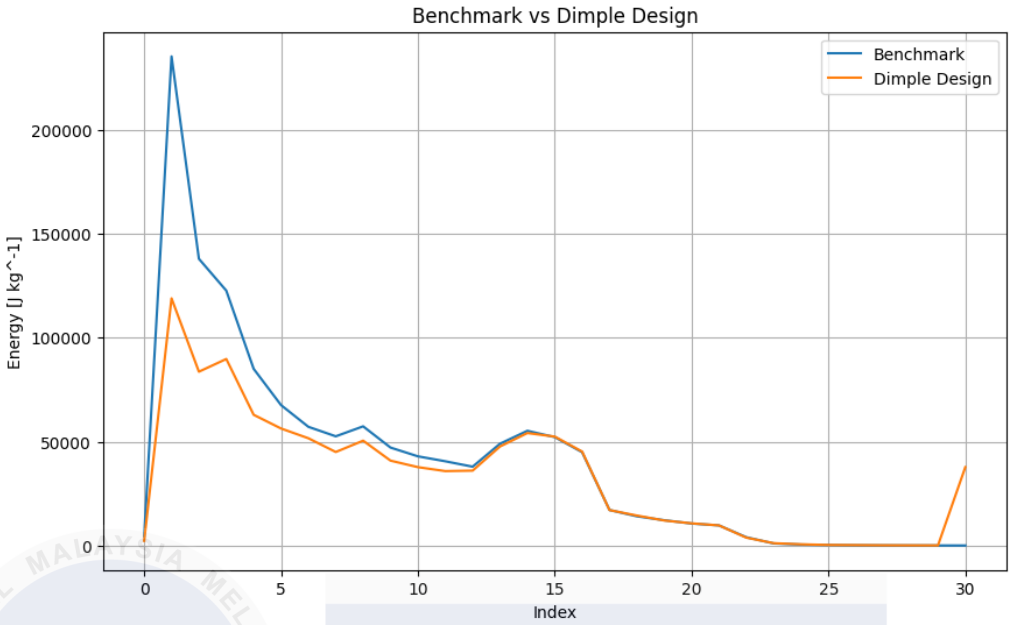

Figure 4.8 Graph of Comparison between Benchmark & Dimple Energy

The energy values for the Dimple Design and the Benchmark are plotted on the graph across several indices. The data points' index is shown on the x-axis, while the energy values are shown on the y-axis

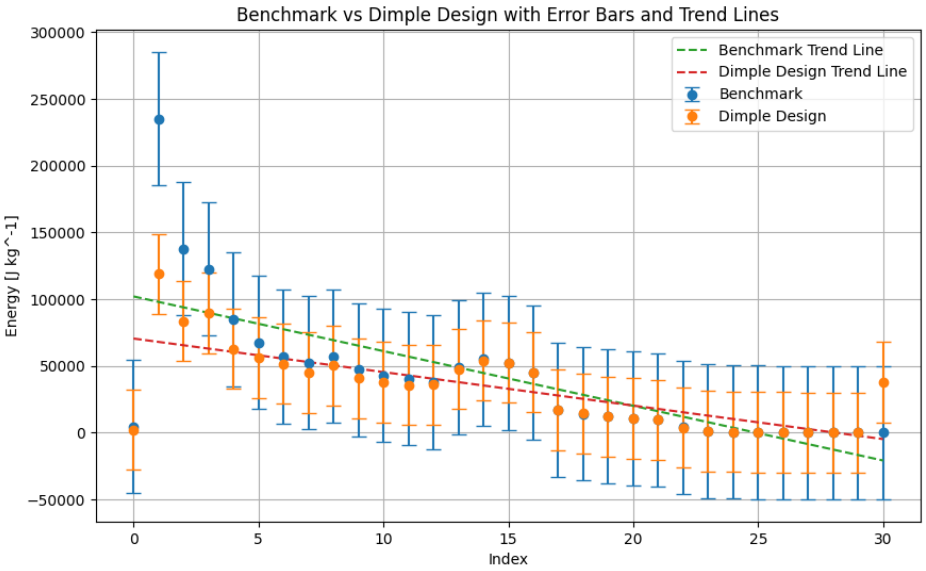

Figure 4.9 Trendline of Benchmark & Dimple Design

The graph illustrates significant variations in the context of TKE by visually comparing the energy figures for the Benchmark and Dimple Design. The Dimple Design has a number of noteworthy advantages over the Benchmark design, which typically shows greater energy ratings. A stable level of turbulent kinetic energy is shown by the Dimple Design's more constant energy values with less variability and standard deviation. Because it guarantees consistent energy distribution and reduces fluctuations that could impair efficiency, this stability is essential for applications needing dependable and predictable performance.

Furthermore, compared to the Benchmark, the Dimple Design's trend line displays a more steady decline in energy values over time. This suggests that the Dimple Design performs better over an extended period of time, giving it a more robust and dependable choice for applications requiring persistent turbulent kinetic energy. The Dimple Design's steady and reliable turbulent flow can improve heat transfer efficiency, encouraging more efficient fluid mixing and enhancing system performance.

Table 4.3 Significant Value of TKE Result

Significant of TKE	Benchmark	Dimple
Mean	4.07 e 4 J/kg	3.29 e 4 J/kg
Median	3.80 e 4 J/kg	3.61 e 4 J/kg
Standard Deviation	4.99 e 4 J/kg	3.01 e 4 J/kg
T test	0.729	
P value	0.469	
Wilcoxon Test	120.0	
P value	0.011	

To provide a deeper understanding of the data, the mean, median, and standard deviation for both the Benchmark and Dimple Design were calculated. For the Benchmark, the mean is 4.07 e 4 J/kg, the median is 3.80 e 4 J/kg, and the standard deviation is 4.99 e 4 J/kg. For the Dimple Design, the mean is 3.29 e 4 J/kg, the median is 3.61 e 4 J/kg, and the standard deviation is 3.01 e 4 J/kg.

. For the t-test, a p-value of 0.469 means there's no significant difference between the two designs, assuming the data follows a normal distribution. However, the Wilcoxon test, with a p-value of 0.011, indicates a significant difference without needing the data to be normally distributed. This suggests that the Dimple Design's energy values are distinct from the Benchmark's, highlighting the importance of choosing the right statistical test based on the data's characteristics. With the p-value Wilcoxon of 0.011 it also proofs that it suits the analysis which is to use non parametric test.

. The standard deviation is used to calculate the energy measurements' variability, which is shown by the error bars. Higher variability in the energy measurements is indicated by the relatively long error bars for the Benchmark data points, which implies that the energy values for the Benchmark design are more widely distributed. The Dimple Design's error bars, on the other hand, are shorter, suggesting less fluctuation and more stable energy readings.

Furthermore, at the 5% significance level, the statistical analysis's p-value indicates that the Benchmark and Dimple Design data sets differ significantly. This indicates that the variations in energy values and variability that we observe are statistically significant.

4.4.1.2 Significance of the Results

The energy figures for the Benchmark and Dimple Design are compared in the graph, which also highlights some significant variations in TKE and their potential effects on drag reduction. The Dimple Design's more constant energy values with reduced variability and standard deviation are among its most notable features. This indicates that the Dimple Design keeps the turbulent kinetic energy constant, which is crucial for applications requiring consistent and dependable performance. More consistent and dependable outcomes may result from this stability, particularly if dimples are used on the Ahmed body's upper surfaces.

An added benefit of the Dimple Design is that, in contrast to the Benchmark, its energy values decline more gradually over time. According to this, the Dimple Design is a more dependable and long-lasting option for applications requiring consistent performance. This implies that maintaining a constant TKE for the Ahmed body can aid in lowering drag and increasing aerodynamic efficiency. The Dimple Design's steady turbulent flow can improve boundary layer mixing, lowering drag and flow separation.

4.4.2 TKE Contour Plane

TKE distributions for a benchmark scenario and a dimple design are depicted in the photographs. The TKE strength is represented by a color scale, where blue denotes less turbulence and red denotes more.

The dimpled surface typically has lower TKE values than the smooth surface, as may be seen from Figure 4.10. This implies that the flow characteristics are considerably altered by the addition of dimples to the surface, resulting in a less turbulent flow.

High TKE zones are specifically visible on the smooth surface's leading and trailing edges, most likely as a result of flow separation and elevated shear stresses. Conversely, the dimpled surface exhibits reduced TKE in these crucial regions. The TKE is significantly lower inside the dimples, suggesting that the dimples aid in flow mixing and turbulence intensity reduction.

In general, the pictures indicate that, in contrast to the smooth surface, the dimpled shape produces a more stable and less turbulent flow. Applications such as lowering drag in aerodynamic systems will be significantly impacted by this.

Turbulence Kinetic Energy	
Benchmark	Dimple Design
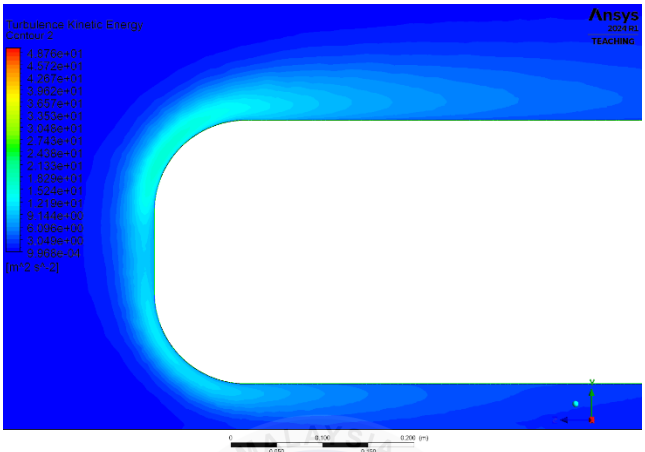 Side View of Ahmed Body	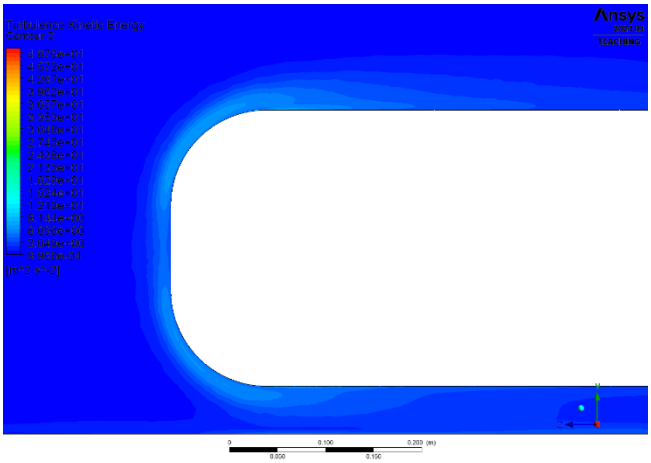 Side View of Ahmed Body
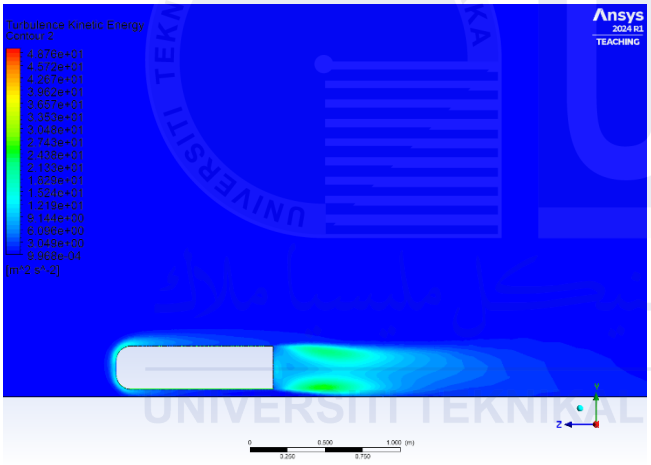 Side View of Ahmed Body (Zoom Out)	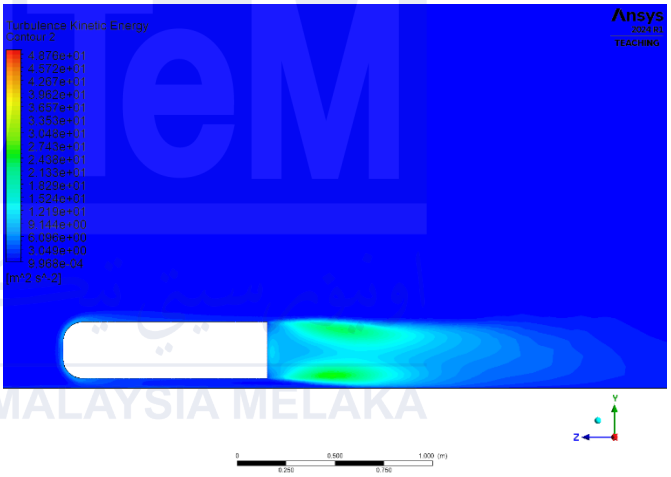 Side View of Ahmed Body (Zoom Out)
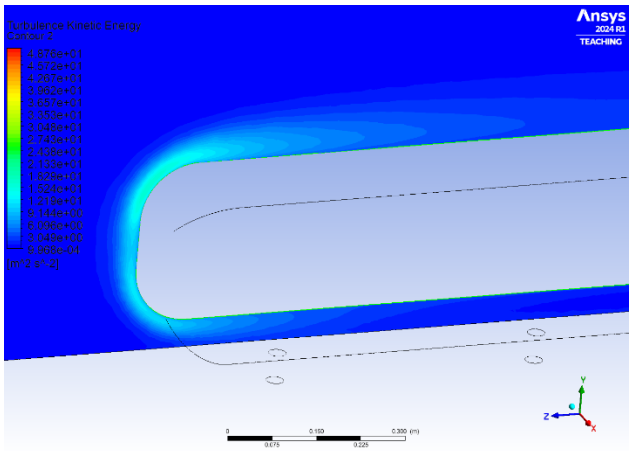 Isometric View of Ahmed Body	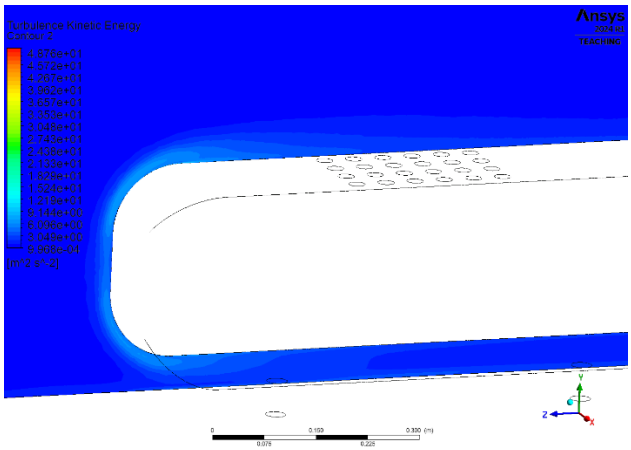 Isometric View of Ahmed Body

Figure 4.10 Comparison of TKE Contour Plane

4.4.3 TKE Contour Graph

The distribution of TKE, a crucial characteristic for comprehending and enhancing aerodynamic performance, is shown in detail in Figure 4.11 The flow's intricacy is revealed by TKE, a measurement of the energy connected to turbulent fluctuations. Intense turbulence is indicated by high TKE zones, which are frequently seen near barriers or in places with notable flow gradients. This is harmful because it increases drag and energy dissipation. Low TKE zones, on the other hand, indicate efficient and smooth flow and are usually found in streamlined areas or areas far from disruptions.

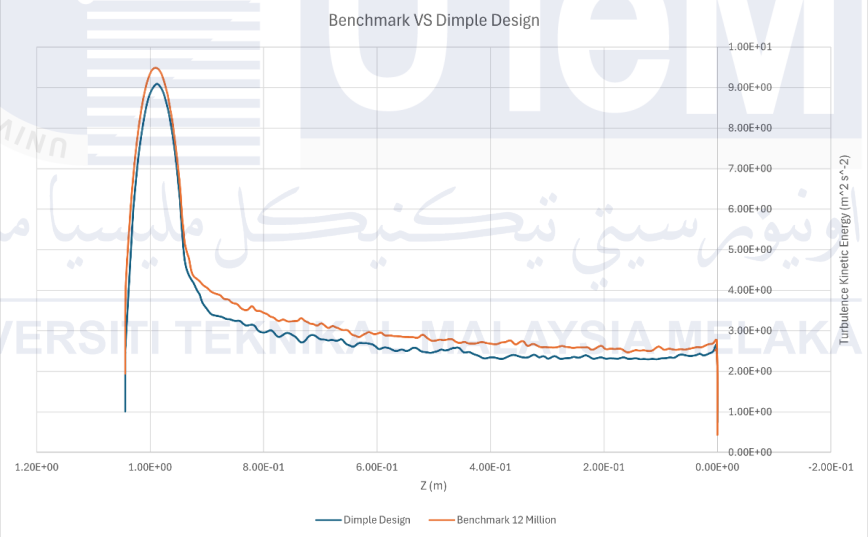

Figure 4.11 TKE distribution

One important finding from Figure 4.11 is the dimple design's steady decrease in TKE values as compared to the benchmark. Because the dimples affect the flow in a way that encourages more ordered and less turbulent flow patterns, there is a noticeable decrease in turbulence. The benchmark design, on the other hand, lacks these dimples and is subject to higher levels of turbulence, which results in increased drag and energy losses.

Moreover, mesh resolution has a significant impact on TKE visualization accuracy. A more realistic depiction of the TKE distribution is achieved by finer meshes, which are able to capture smaller turbulent features that coarser meshes could overlook. Because it enables a more thorough comprehension of flow behavior and the identification of tactics to further reduce turbulence, this level of information is essential for in-depth study and optimization.

Put it all up, Figure 4.11 offers important information about the dimple design's aerodynamic benefits. When compared to the benchmark, the dimples successfully minimize turbulence, improving flow characteristics and possibly reducing drag, as the TKE distribution visualization makes evident. This study emphasizes how crucial careful mesh analysis and TKE visualization are to directing design optimization and attaining optimal aerodynamic performance.

Chapter 5

Conclusion and Future Recommendations

5.1 Conclusion

The purpose of the research was to evaluate the impact of dimples on drag and TKE, compare the aerodynamic performance of smooth-surface and dimple-augmented Ahmed bodies, and validate the results using CFD. By lowering wake vortices and stabilizing boundary layer attachment, dimpled surfaces enhanced flow patterns and decreased drag. The potential of dimples to increase aerodynamic efficiency was validated by localized turbulence reduction, even though statistical studies revealed no discernible difference in mean TKE.

Thorough grid sensitivity analysis and elaborate turbulence modeling were used in the CFD validation process, which confirmed accurate and dependable results. Compliance with aerodynamic standards demonstrated the simulation process's stability to evaluate aerodynamic performance and increased trust in the study's results.

In order to delay flow separation and stabilize airflow, dimples altered the distribution of TKE by enhancing turbulence in some areas and decreasing it in others. The advantages of surface alterations were demonstrated by qualitative analysis, which revealed decreased drag and improved aerodynamic performance even though mean TKE differences were statistically minimal.

5.2 Future Recommendations

Future research should examine how to maximize drag reduction and turbulence management by optimizing the geometry, size, and positioning of dimples. Aerodynamic efficiency could be greatly increased by determining the best combinations. To obtain a thorough grasp of the aerodynamic performance in dynamic settings, transient CFD simulations should also be carried out under real-world circumstances, such as crosswinds, fluctuating speeds, and transient wake behavior.

It is also highly recommended to do experimental validation using wind tunnel testing on full-size or scaled-up Ahmed body models. This would address any assumptions made during the simulations and offer tangible confirmation of the computational results. In order to investigate more aerodynamic advantages, surface alterations could also be extended to regions like the vehicle's roof, back, and underbody.

Alongside aerodynamic efficiency, future studies should measure the useful benefits of dimple-augmented designs, like increased fuel economy and lower carbon emissions. The wider effects of dimpled surfaces would be better-understood thanks to these evaluations, especially in relation to their contribution to environmentally friendly and energy-efficient transportation options. The car industry might fully grasp the promise of dimple augmentation by addressing these factors.

REFERENCES

Adrian, R. (1991). Particle-Imaging Techniques For Experimental Fluid-Mechanics. *Annual Review of Fluid Mechanics*, *23*, 261–304. https://doi.org/10.1146/annurev.fluid.23.1.261

Ahmed, S. R., Ramm, G., & Faltin, G. (1984). Some Salient Features of the Time -Averaged Ground Vehicle Wake. *SAE Transactions*, *93*, 473–503. http://www.jstor.org/stable/44434262

An_Introduction_to_Computational_Fluid_D. (n.d.).

BALACHANDAR, S., MITTAL, R., & NAJJAR, F. M. (1997). Properties of the mean recirculation region in the wakes of two-dimensional bluff bodies. *Journal of Fluid Mechanics*, *351*, 167–199. https://doi.org/DOI: 10.1017/S0022112097007179

Barlow, J. B., Rae, W. H., Pope, A., & Pope, A. (1999). *Low-speed wind tunnel testing*. Wiley.

Chatterjee, D., Mazumder, B. S., Ghosh, S., & Debnath, K. (2021). Turbulent flow characteristics over forward-facing obstacle. *Journal of Turbulence*, *22*(3), 141 – 179. https://doi.org/10.1080/14685248.2020.1854461

citations-20240610T140056. (n.d.).

Downs, S. H., & Black, N. (1998). The feasibility of creating a checklist for the assessment of the methodological quality both of randomised and non-randomised studies of health care interventions. *Journal of Epidemiology and Community Health*, *52*(6), 377. https://doi.org/10.1136/jech.52.6.377

Fang, L., Zhao, H., Ni, W., Fang, J., & Lu, L. (2019). Non-equilibrium turbulent phenomena in the flow over a backward-facing ramp. *Applied Mathematics and Mechanics (English Edition)*, *40*(2), 215 – 236. https://doi.org/10.1007/s10483-019-2428-6

Farghaly, M. B., Sarhan, H. H., & Abdelghany, E. S. (2023). Aerodynamic Performance Enhancement of a Heavy Trucks using Experimental and Computational Investigation. *CFD Letters*, *15*(8), 73 – 94. https://doi.org/10.37934/cfdl.15.8.7394

Feng, Y., & Zhang, H. (2022). Aerodynamic drag reduction device based on rear wind energy harvesting; [基于车尾风能回收的气动减阻装置]. *Hangkong Xuebao/Acta Aeronautica et Astronautica Sinica*, *43*. https://doi.org/10.7527/S1000-6893.2022.27740

Ferziger, J. H., & Peric, M. (n.d.). *Computational Methods for Fluid Dynamics*.

Fundamentals_of_Aerodynamics. (n.d.).

Gong, Z., Duan, Y., Chen, X., Li, D., & Fu, X. (2023). Statistical behavior of wall-attached motions in open- and closed-channel flows via direct numerical simulation. *Physics of Fluids*, *35*(4). https://doi.org/10.1063/5.0144392

Grant, M. J., & Booth, A. (2009). A typology of reviews: an analysis of 14 review types and associated methodologies. *Health Information & Libraries Journal*, *26*(2), 91–108. https://doi.org/https://doi.org/10.1111/j.1471-1842.2009.00848.x

Hamizi, I. B., & Khan, S. A. (2019). Aerodynamics investigation of delta wing at low reynold's number. *CFD Letters*, *11*(2), 32 – 41. https://www.scopus.com/inward/record.uri?eid=2-s2.0-85062830466&partnerID=40&md5=0a8b652517e8efc25e2cc8773e49784c

Hesse, F., & Morgans, A. S. (2021). Simulation of wake bimodality behind squareback bluff-bodies using LES. *Computers and Fluids*, *223*. https://doi.org/10.1016/j.compfluid.2021.104901

Hu, X.-J., Guo, P., Hui, Z., Yu, T.-M., Yang, C.-H., Xiao, Y., Wang, J.-Y., Li, J.-X., & Miao, Y.-X. (2019). Effect of porous media on the aerodynamic characteristics of van-body truck; [多孔介质对厢式货车气动特性的影响]. *Jilin Daxue Xuebao (Gongxueban)/Journal of Jilin*

University (Engineering and Technology Edition), *49*(2), 345 – 350. https://doi.org/10.13229/j.cnki.jdxbgxb20171299

Hwang, Y., & Eckhardt, B. (2020). Attached eddy model revisited using a minimal quasi-linear approximation. *Journal of Fluid Mechanics*, *894*. https://doi.org/10.1017/jfm.2020.285

Jaffar, H., Al-Sadawi, L., Khudhair, A., & Biedermann, T. (2023). Aerodynamics improvement of DU97-W-300 wind turbine flat-back airfoil using slot-induced air jet. *International Journal of Thermofluids*, *17*. https://doi.org/10.1016/j.ijft.2022.100267

Javanappa, S. K., & Narasimhamurthy, V. D. (2021). Turbulent plane Couette flow with a roughened wall. *Physical Review Fluids*, *6*(10). https://doi.org/10.1103/PhysRevFluids.6.104609

Jin, W. (2021). Cavitation generation and inhibition. I. Dominant mechanism of turbulent kinetic energy for cavitation evolution. *AIP Advances*, *11*(6). https://doi.org/10.1063/5.0050231

Kadivar, M., Tormey, D., & McGranaghan, G. (2021). A review on turbulent flow over rough surfaces: Fundamentals and theories. *International Journal of Thermofluids*, *10*. https://doi.org/10.1016/j.ijft.2021.100077

Kitchenham, B. (2004). *Procedures for Performing Systematic Reviews*.

Koppa Shivanna, N., Ranjan, P., & Clement, S. (2021). The effect of rear cavity modifications on the drag and flow field topology of a Square Back Ahmed Body. *PROCEEDINGS OF THE INSTITUTION OF MECHANICAL ENGINEERS PART D-JOURNAL OF AUTOMOBILE ENGINEERING*, *235*(7), 1849–1863. https://doi.org/10.1177/0954407021990918

Leschziner, M. A. (2020). Friction-Drag Reduction by Transverse Wall Motion - A Review. *Journal of Mechanics*, *36*(5), 649 – 663. https://doi.org/10.1017/jmech.2020.31

Liu, J., Zhao, P., Lei, M., Yang, S., & Nemati, H. (2020). Numerical investigation of spatial-developing turbulent heat transfer in forced convections at different supercritical pressures.

International Journal of Heat and Mass Transfer, *159*. https://doi.org/10.1016/j.ijheatmasstransfer.2020.120128

Liu, Y., Stoesser, T., & Fang, H. (2022). Effect of secondary currents on the flow and turbulence in partially filled pipes. *JOURNAL OF FLUID MECHANICS*, *938*. https://doi.org/10.1017/jfm.2022.141

Lu, H., Yang, Y., Guo, S., Pang, W., Yang, F., & Zhong, J. (2019). Control of corner separation via dimpled surface for a highly loaded compressor cascade under different inlet Mach number. *Aerospace Science and Technology*, *85*, 48 – 60. https://doi.org/10.1016/j.ast.2018.11.054

Ludwig Prandtl, "Motion of Fluids with Very Little Viscosity" (1904). (n.d.). https://germanhistory-intersections.org/en/knowledge-and-education/ghis:document-202

Marimuthu, S., & Chinnathambi, D. (2020). Computational analysis of biomimetic butterfly valve. *Bioinspired, Biomimetic and Nanobiomaterials*, *9*(4), 223 – 232. https://doi.org/10.1680/jbibn.20.00027

Martyn-St James, M., Clowes, M., & Sutton, A. (2021). *Systematic Approaches to a Successful Literature Review*. SAGE Publications Ltd. http://digital.casalini.it/9781529759648

Menter, F. ~R. (1994). Two-equation eddy-viscosity turbulence models for engineering applications. *AIAA Journal*, *32*(8), 1598–1605. https://doi.org/10.2514/3.12149

Moher David AND Liberati, A. A. N. D. T. J. A. N. D. A. D. G. A. N. D. T. P. G. (2009). Preferred Reporting Items for Systematic Reviews and Meta-Analyses: The PRISMA Statement. *PLOS Medicine*, *6*(7), 1–6. https://doi.org/10.1371/journal.pmed.1000097

Mondal, A., Chatterjee, S., Tariang, A. M., Raj, L. P., & Debnath, K. (2023). Numerical investigation of on-demand fluidic winglet aerodynamic performance and turbulent characterization of a low

aspect ratio wing. *Advances in Aircraft and Spacecraft Science*, *10*(2), 107 – 125. https://doi.org/10.12989/aas.2023.10.2.107

Montazeri, H., & Blocken, B. (2013). CFD simulation of wind-induced pressure coefficients on buildings with and without balconies: Validation and sensitivity analysis. *Building and Environment*, *60*, 137–149. https://doi.org/https://doi.org/10.1016/j.buildenv.2012.11.012

Naim, M. S., & Baig, M. F. (2019). Turbulent drag reduction in Taylor-Couette flows using different super-hydrophobic surface configurations. *Physics of Fluids*, *31*(9). https://doi.org/10.1063/1.5116316

Nguyen, H. T., Chang, K., Lee, S.-W., Ryu, J., & Kim, M. (2022). Numerical Prediction of Turbulent Drag Reduction with Different Solid Fractions and Distribution Shapes over Superhydrophobic Surfaces. *Energies*, *15*(18). https://doi.org/10.3390/en15186645

Page, M. J., McKenzie, J. E., Bossuyt, P. M., Boutron, I., Hoffmann, T. C., Mulrow, C. D., Shamseer, L., Tetzlaff, J. M., Akl, E. A., Brennan, S. E., Chou, R., Glanville, J., Grimshaw, J. M., Hróbjartsson, A., Lalu, M. M., Li, T., Loder, E. W., Mayo-Wilson, E., McDonald, S., … Moher, D. (2021). The PRISMA 2020 statement: an updated guideline for reporting systematic reviews. *BMJ*, *372*. https://doi.org/10.1136/bmj.n71

Pan, Q., Xiang, H., Wang, Z., Andersson, H. I., & Zhao, L. (2020). Kinetic energy balance in turbulent particle-laden channel flow. *Physics of Fluids*, *32*(7). https://doi.org/10.1063/5.0012570

Panda, J. P., & Warrior, H. V. (2022). Data-Driven Prediction of Complex Flow Field Over an Axisymmetric Body of Revolution Using Machine Learning. *Journal of Offshore Mechanics and Arctic Engineering*, *144*(6). https://doi.org/10.1115/1.4055280

Paul, A. R., Jain, A., & Alam, F. (2019). Drag Reduction of a Passenger Car Using Flow Control Techniques. *International Journal of Automotive Technology*, *20*(2), 397 – 410. https://doi.org/10.1007/s12239-019-0039-2

Petticrew, M., & Roberts, H. (2006). Systematic reviews in the social sciences: A practical guide. In *Systematic reviews in the social sciences: A practical guide.* Blackwell Publishing. https://doi.org/10.1002/9780470754887

Ramirez-Pastran, J., & Duque-Daza, C. (2019). On the prediction capabilities of two SGS models for large-eddy simulations of turbulent incompressible wall-bounded flows in OpenFOAM. *Cogent Engineering*, *6*(1). https://doi.org/10.1080/23311916.2019.1679067

Ricco, P., Skote, M., & Leschziner, M. A. (2021). A review of turbulent skin-friction drag reduction by near-wall transverse forcing. *Progress in Aerospace Sciences*, *123*. https://doi.org/10.1016/j.paerosci.2021.100713

Sharma, V., & Dutta, S. (2023). Experimental and Numerical Investigation of Bio-Inspired Riblet for Drag Reduction. *JOURNAL OF FLUIDS ENGINEERING-TRANSACTIONS OF THE ASME*, *145*(2). https://doi.org/10.1115/1.4056185

Shea, B. J., Reeves, B. C., Wells, G., Thuku, M., Hamel, C., Moran, J., Moher, D., Tugwell, P., Welch, V., Kristjansson, E., & Henry, D. A. (2017). AMSTAR 2: a critical appraisal tool for systematic reviews that include randomised or non-randomised studies of healthcare interventions, or both. *BMJ*, *358*. https://doi.org/10.1136/bmj.j4008

SPALART, P., & ALLMARAS, S. (1992). A one-equation turbulence model for aerodynamic flows. In *30th Aerospace Sciences Meeting and Exhibit*. American Institute of Aeronautics and Astronautics. https://doi.org/doi:10.2514/6.1992-439

Stephen B Pope. (2001). Turbulent Flows. *Measurement Science and Technology*, *12*(11), 2020. https://doi.org/10.1088/0957-0233/12/11/705

Toloui, M., Abraham, A., & Hong, J. (2019). Experimental investigation of turbulent flow over surfaces of rigid and flexible roughness. *Experimental Thermal and Fluid Science*, *101*, 263 – 275. https://doi.org/10.1016/j.expthermflusci.2018.10.026

Touber, E. (2019). Small-scale two-dimensional turbulence shaped by bulk viscosity. *Journal of Fluid Mechanics*, *875*, 974 – 1003. https://doi.org/10.1017/jfm.2019.531

Tranfield, D., Denyer, D., & Smart, P. (2003). Towards a Methodology for Developing Evidence-Informed Management Knowledge by Means of Systematic Review. *British Journal of Management*, *14*(3), 207–222. https://doi.org/https://doi.org/10.1111/1467-8551.00375

Vashishtha, S., Samuel, R., Chatterjee, A. G., Samtaney, R., & Verma, M. K. (2019). Large eddy simulation of hydrodynamic turbulence using renormalized viscosity. *Physics of Fluids*, *31*(6). https://doi.org/10.1063/1.5096335

Virgilio, M., Dedeyne, J. N., Van Geem, K. M., Marin, G. B., & Arts, T. (2020). Dimples in turbulent pipe flows: experimental aero-thermal investigation. *International Journal of Heat and Mass Transfer*, *157*. https://doi.org/10.1016/j.ijheatmasstransfer.2020.119925

Wang, H., Fan, Y., Yan, Z., & Li, W. (2023). Direct numerical simulations of turbulent flow over the converging and diverging riblets. *Physics of Fluids*, *35*(7). https://doi.org/10.1063/5.0154866

Wang, J., Minelli, G., Dong, T., He, K., & Krajnović, S. (2020). Impact of the bogies and cavities on the aerodynamic behaviour of a high-speed train. An IDDES study. *Journal of Wind Engineering and Industrial Aerodynamics*, *207*. https://doi.org/10.1016/j.jweia.2020.104406

Wang, Q.-X., Fan, Z.-Y., Yue, J.-H., Bai, J.-X., Cheng, X.-Q., Tian, H.-P., & Jiang, N. (2024). The spatial-temporal multi-scale characteristics of turbulent kinetic energy and typical structures in

turbulent boundary layer. *Acta Mechanica Sinica/Lixue Xuebao*, *40*(3). https://doi.org/10.1007/s10409-023-23254-x

Wang, X., He, D., Liu, J., Li, H., Guo, C., & Jiang, M. (2023). Influence of cage lifting piston effect on drift airflow in main intake shaft; [主进风竖井内罐笼提升活塞效应对平巷风流的影响]. *Meitan Xuebao/Journal of the China Coal Society*, *48*, 159 – 170. https://doi.org/10.13225/j.cnki.jccs.2022.1175

Wang, Y., Cao, L., Cheng, Z., Blanpain, B., & Guo, M. (2021). Mathematical methodology and metallurgical application of turbulence modelling: A review. *Metals*, *11*(8). https://doi.org/10.3390/met11081297

Wei, M., Cheng, N.-S., Chiew, Y.-M., & Yang, F. (2019). Vortex evolution within propeller induced scour hole around a vertical quay wall. *Water (Switzerland)*, *11*(8). https://doi.org/10.3390/w11081538

Wilcox, D. C. (2006). *Turbulence modeling for CFD*. DCW Industries.

Xia, Y., Lin, Z., Pan, D., & Yu, Z. (2021). Turbulence modulation by finite-size heavy particles in a downward turbulent channel flow. *Physics of Fluids*, *33*(6). https://doi.org/10.1063/5.0053540

Yagmur, S., Dogan, S., Aksoy, M. H., & Goktepeli, I. (2020). Turbulence modeling approaches on unsteady flow structures around a semi-circular cylinder. *Ocean Engineering*, *200*. https://doi.org/10.1016/j.oceaneng.2020.107051

Ying, L., Shiqing, L., Lingwei, Z., & Hanfeng, W. (2019). Control of the VIV of a cantilevered square cylinder with free-end suction. *Wind and Structures, An International Journal*, *29*(1), 75 – 84. https://doi.org/10.12989/was.2019.29.1.075

Yoo, D., & Paik, J. (2020). An evaluation of wall functions for RANS computation of turbulent flows. *Journal of Korea Water Resources Association*, *53*(1), 1 – 13. https://doi.org/10.3741/JKWRA.2020.53.1.1

Yousif, M. Z., Yang, Y., Zhou, H., Mohammadikarachi, A., Yu, L., Zhang, M., & Lim, H.-C. (2024). Flow Control Over a Finite Wall-Mounted Square Cylinder by Using Multiple Plasma Actuators. *Journal of Fluids Engineering, Transactions of the ASME*, *146*(6). https://doi.org/10.1115/1.4064387

Yudianto, A., Adiyasa, I. W., & Yudantoko, A. (2021). Aerodynamics of bus platooning under crosswind. *Automotive Experiences*, *4*(3), 119 – 130. https://doi.org/10.31603/ae.5298

Yunqing, G., Tao, L., Jiegang, M., Zhengzan, S., & Peijian, Z. (2017). Analysis of Drag Reduction Methods and Mechanisms of Turbulent. *Applied Bionics and Biomechanics*, *2017*(1), 6858720. https://doi.org/https://doi.org/10.1155/2017/6858720

ZHANG, Y., YAN, C., CHEN, H., & YIN, Y. (2020). Study of riblet drag reduction for an infinite span wing with different sweep angles. *Chinese Journal of Aeronautics*, *33*(12), 3125 – 3137. https://doi.org/10.1016/j.cja.2020.05.015

APPENDICES

APPENDIX A – Gaant Chart of PSM 1

Task \ Week		W1	W2	W3	W4	W5	W6	W7	W8 (Mid Term Break)	W9	W10	W11	W12	W13	W14
PSM Title Registration	P														
	A														
Project Briefing	P														
	A														
Research About the Title	P														
	A														
Literature Review (Chp.2)	P														
	A														
Method for the Project	P														
	A														
Methodology (Chp.3)	P														
	A														
Benchmark Design	P														
	A														
Introduction (Chp.1)	P														
	A														
Writing Full Report	P														
	A														
Submit draft to Supervisor	P														
	A														
Project Presentation	P														
	A														

APPENDIX B - Gaant Chart of PSM 2

Task \ Week		W1	W2	W3	W4	W5	W6	W7	W8	W9	W10	W11	W12	W13	W14
PSM 2 Briefing	P														
	A														
Running Dimple Design analysis	P														
	A														
Data gathering for Dimple Design Analysis	P														
	A														
Data gathering for Dimple Design Analysis	P														
	A														
BDP Workshop Series: AI Tools in Thesis Writing	P														
	A														
BDP Workshop Series: Statistical Data Analysis for BDP	P														
	A														
Talent Enhancement 2024	P														
	A														

BDP Workshop Series: Do's and Don’ts in writing result and discussion	P														
	A														
Chapter 4 checking	P														
	A														
Report Writing	P														
	A														
PSM 2 Report Submission to Supervisor	P														
	A														
Report Submission to Panel	P														
	A														
Presentation	P														
	A														

APPENDIX C – TABLE OF PRESSURE CONTOUR PLANE

Table Difference of Pressure Benchmark and Dimple Design

Pressure | 12 Mil. Element	Benchmark	Dimple Design
Plane 1	4.236e+5 [Pa]	4.423e+5 [Pa]
Plane 2	-3.433e+6 [Pa]	-3.494e+6 [Pa]
Plane 3	-2.109e+6 [Pa]	-1.977e+6 [Pa]
Plane 4	-1.531e+6 [Pa]	-1.415e+6 [Pa]
Plane 5	-9.114e+5 [Pa]	-8.216e+5 [Pa]
Plane 6	-6.898e+5 [Pa]	-5.774e+5 [Pa]
Plane 7	-5.597e+5 [Pa]	-4.466e+5 [Pa]
Plane 8	-4.783e+5 [Pa]	-4.033e+5 [Pa]
Plane 9	-5.758e+5 [Pa]	-5.030e+5 [Pa]
Plane 10	-5.799e+5 [Pa]	-5.051e+5 [Pa]
Plane 11	-6.522e+5 [Pa]	-5.818e+5 [Pa]
Plane 12	-8.552e+5 [Pa]	-7.893e+5 [Pa]

Table Difference of Velocity Benchmark and Dimple Design

Velocity | 12 Mil. Element	Benchmark	Dimple Design
Plane 1	1.812e+5 [m s^-1]	1.763e+5 [m s^-1]
Plane 2	6.702e+5 [m s^-1]	6.770e+5 [m s^-1]
Plane 3	5.343e+5 [m s^-1]	5.339e+5 [m s^-1]
Plane 4	4.886e+5 [m s^-1]	4.923e+5 [m s^-1]
Plane 5	4.713e+5 [m s^-1]	4.686e+5 [m s^-1]
Plane 6	4.619e+5 [m s^-1]	4.535e+5 [m s^-1]
Plane 7	4.540e+5 [m s^-1]	4.449e+5 [m s^-1]
Plane 8	4.541e+5 [m s^-1]	4.457e+5 [m s^-1]
Plane 9	4.420e+5 [m s^-1]	4.346e+5 [m s^-1]
Plane 10	4.585e+5 [m s^-1]	4.517e+5 [m s^-1]
Plane 11	4.607e+5 [m s^-1]	4.532e+5 [m s^-1]
Plane 12	4.587e+5 [m s^-1]	4.475e+5 [m s^-1]
Plane 13	2.116e+5 [m s^-1]	2.073e+5 [m s^-1]
Plane 14	2.181e+5 [m s^-1]	2.129e+5 [m s^-1]
Plane 15	2.266e+5 [m s^-1]	2.209e+5 [m s^-1]
Plane 16	2.266e+5 [m s^-1]	2.240e+5 [m s^-1]
Plane 17	2.278e+5 [m s^-1]	2.251e+5 [m s^-1]
Plane 18	1.677e+5 [m s^-1]	1.647e+5 [m s^-1]
Plane 19	1.669e+5 [m s^-1]	1.656e+5 [m s^-1]
Plane 20	1.715e+5 [m s^-1]	1.668e+5 [m s^-1]
Plane 21	1.716e+5 [m s^-1]	1.680e+5 [m s^-1]
Plane 22	1.732e+5 [m s^-1]	1.676e+5 [m s^-1]
Plane 23	9.679e+4 [m s^-1]	9.160e+4 [m s^-1]
Plane 24	4.809e+4 [m s^-1]	4.404e+4 [m s^-1]
Plane 25	3.335e+4 [m s^-1]	3.034e+4 [m s^-1]
Plne 26	2.744e+4 [m s^-1]	2.305e+4 [m s^-1]
Plane 27	2.381e+4 [m s^-1]	1.909e+4 [m s^-1]
Plane 28	2.137e+4 [m s^-1]	1.604e+4 [m s^-1]
Plane 29	1.896e+4 [m s^-1]	1.368e+4 [m s^-1]
Plane 30	1.784e+4 [m s^-1]	1.202e+4 [m s^-1]
Plane 31	1.692e+4 [m s^-1]	4.532e+5 [m s^-1]

Table 4.16 Comparison of TKE with Dimple Design

TKE (J kg^{-1}) | 12 Mil. Element	Benchmark	Dimple Design
Plane 1	4.498e+3 [J kg^ -1]	2.307e+3 [J kg^ -1]
Plane 2	2.352e+5 [J kg^ -1]	1.189e+5 [J kg^ -1]
Plane 3	1.379e+5 [J kg^ -1]	8.363e+4 [J kg^ -1]
Plane 4	1.226e+5 [J kg^ -1]	8.974e+4 [J kg^ -1]
Plane 5	8.501e+4 [J kg^ -1]	6.292e+4 [J kg^ -1]
Plane 6	6.758e+4 [J kg^ -1]	5.633e+4 [J kg^ -1]
Plane 7	5.713e+4 [J kg^ -1]	5.163e+4 [J kg^ -1]
Plane 8	5.257e+4 [J kg^ -1]	4.503e+4 [J kg^ -1]
Plane 9	5.736e+4 [J kg^-1]	5.047e+4 [J kg^-1]
Plane 10	4.716e+4 [J kg^ -1]	4.088e+4 [J kg^ -1]
Plane 11	4.295e+4 [J kg^ -1]	3.775e+4 [J kg^ -1]
Plane 12	4.057e+4 [J kg^ -1]	3.585e+4 [J kg^ -1]
Plane 13	3.797e+4 [J kg^ -1]	3.607e+4 [J kg^ -1]
Plane 14	4.900e+4 [J kg^ -1]	4.767e+4 [J kg^ -1]
Plane 15	5.522e+4 [J kg^ -1]	5.414e+4 [J kg^ -1]
Plane 16	5.219e+4 [J kg^ -1]	5.244e+4 [J kg^ -1]
Plane 17	4.494e+4 [J kg^ -1]	4.524e+4 [J kg^ -1]
Plane 18	1.716e+4 [J kg^ -1]	1.711e+4 [J kg^ -1]
Plane 19	1.412e+4 [J kg ^ -1]	1.448e+4 [J kg ^ -1]
Plane 20	1.223e+4 [J kg^ -1]	1.211e+4 [J kg^ -1]
Plane 21	1.065e+4 [J kg^ -1]	1.073e+4 [J kg^ -1]
Plane 22	9.746e+3 [J kg^ -1]	9.744e+3 [J kg^ -1]
Plane 23	4.053e+3 [J kg^ -1]	3.855e+3 [J kg^ -1]
Plane 24	1.079e+3 [J kg^ -1]	1.188e+3 [J kg^ -1]
Plane 25	5.224e+2 [J kg^ -1]	6.534e+2 [J kg^ -1]
Plane 26	3.229e+2 [J kg^ -1]	3.437e+2 [J kg^ -1]
Plane 27	2.017e+2 [J kg^ -1]	2.678e+2 [J kg^ -1]
Plane 28	1.461e+2 [J kg^ -1]	1.846e+2 [J kg^ -1]
Plane 29	1.102e+2 [J kg^ -1]	1.494e+2 [J kg^ -1]
Plane 30	9.517e+1 [J kg^ -1]	1.260e+2 [J kg^ -1]
Plane 31	8.425e+1 [J kg^ -1]	3.775e+4 [J kg^ -1]